

**Proposed Revisions to Procedures for Testing and Evaluating Radiating Noise  
Sources from Small Firearms, including the ANSI/ASA S12.42-2010  
Procedure**

Sadreddine Sarray, ing.

Thesis submitted to the University of Ottawa in partial fulfilment of the  
requirements for the M.A.Sc. Degree in Electrical and Computer Engineering

Ottawa – Carleton Institute for Electrical and Computer Engineering  
School of Electrical Engineering and Computer Science

University of Ottawa

© Sadreddine Sarray, Ottawa, Canada, 2020

## ABSTRACT

The escalating cost of claims for Noise Induced Hearing Loss (NIHL) in the Canadian Armed Forces (CAF) supports the need to review and upgrade current hearing conservation practices.

The rise of these escalating costs and the need to protect the military personnel when training in extreme noise conditions has initiated an engineering investigation within the Department of National Defence (DND) and in collaboration with the University of Ottawa, to review the existing standards in the field of hearing protection test and evaluation, to propose technical recommendations and to identify the possible technical problems and gaps impacting the quality of the existing procedures.

This study dealt with the estimation of the protection capability of Hearing Protection Devices (HPDs) in the case of high-level impulse noise from small firearms weapons that are a particularly damaging source of noise in military environments, representing an important cause of NIHL.

Testing and evaluation based on a system engineering approach have been used in this work introducing:

- A new testing approach, based on ANSI/ASA S12.42-2010, for testing HPDs when the impulse noise is generated by a small firearm;
- A new evaluation approach for HPD performance, introducing a characterization approach using a sub-band analysis for dealing with impulse noise generated by a small firearm.

The effectiveness of HPDs, taking into account the physiological human limitations induced by Bone Conduction (BC), is computed by using an innovative method attempting to better prevent the risk of NIHL when using small firearms.

# Statement of Originality

This thesis describes the research work that was done by the author at the University of Ottawa for completion of the Master of Applied Science (M.A.Sc) program in Electrical and Computer Engineering. A portion of this research has been reported in the following publication:

Sadreddine Sarray, Ann Nakashima, Hilmi R. Dajani, Martin Bouchard, David Lo, Sebastian Ghinet; **“OCTAVE BAND IMPULSE PEAK INSERTION LOSS: A METHOD TO CHARACTERIZE HEARING PROTECTION DEVICES WHEN FIRING WITH SMALL ARMS”**; 26th International Congress on Sound and Vibration (ICSV26), 8 pages, Montreal, 7-11 July 2019

The results reported in the above-mentioned paper are reflected throughout this thesis. The author performed data analysis, prepared the documents for publication, and made all necessary changes based on feedback from co-authors and paper reviewers.

# Acknowledgements

I would like to express my deepest gratitude to Canada, that provided me with the respect and the freedom that I needed as a human and as a citizen.

I would like to express my deepest gratitude to my supervisors Professor Martin Bouchard and Professor Hilmi Dajani for their continued guidance and valuable support.

Professor Bouchard is very accurate and very knowledgeable, what always pushed me to pick and to absorb his recommendations; his passion and dedication to his work always encouraged me to excel in my studies and to push my limits.

With Professor Bouchard, I was always challenged to develop rigor.

Professor Dajani was able to help me building the foundations of the critical thoughts related to sensory systems modelling and simulation.

With Professor Dajani I was always invited to dare thinking outside of the box.

I would like to express my deepest gratitude to Dr David Lo for his advices and for involving military stakeholders to support this applied research project.

I would like to express my deepest gratitude to my colleagues Mr. Bruno Tardif and MCpl Alexandre Saumure for supporting me with all their best during some of the stressful moments experienced during the last 3 years.

I would like to express my deepest gratitude to all those who provided me with their support and help, because they did trust my capabilities, as an engineer, to bring something new to the soldier. I hope I was able to meet their expectations.

Finally, I would like to express my sincere salutations for those who encountered difficulties understanding my personality. I am inviting them to read the book: “AGURZIL LE DIEU IMPIE” by Tiziri Wuming. This book depicts, in a very nice roman, the Berber or the Amazigh mythology which is completely different from what is known from the Abrahamic heritage.

With a complete faithfulness to my Amazigh way of thought, exploring beyond my intellectual limits was part of the challenge that I’m delivering to Gods during this very short life; hence the work produced in this thesis.

Sadri Sarray, ing.

# Table of Contents

Chapter 1 – INTRODUCTION.....	1
1.1. Motivation and Previous work.....	1
1.2. Objectives and Organization.....	2
1.3. Contributions .....	3
Chapter 2 – SCOPE REVIEW OF THE HEARING PROTECTION DEVICES PERFORMANCE REQUIREMENTS .....	4
2.1. The systems engineering approach .....	4
2.2. Perception of sound.....	6
2.2.1 Frequency Scale:.....	6
2.2.2 Intensity Scale:.....	7
2.2.3 Hearing Thresholds: .....	8
2.3. Impulse noise as a health hazard.....	8
2.4. Methods used for HPD evaluation under impulse noise .....	10
2.5. Discussion.....	11
2.6. Conclusion.....	12
Chapter 3 – REVIEW AND USE OF THE ANSI/ASA S12.42-2010 TESTING STRATEGY WHEN THE IMPULSE NOISE IS GENERATED BY A SMALL FIREARM.....	13
3.1. Introduction .....	13
3.2. Methods.....	15
3.2.1. Characterisation of small firearm radiations.....	16
3.2.1.1. Testing procedure.....	16
3.2.1.2. Data Analysis & Results.....	20
3.2.2. Characterization of Hearing Protection Devices.....	24
3.2.2.1. Testing procedure.....	24
3.2.2.2. Data analysis .....	27
3.2.2.2.1. IPIL calculation when using a sequential test and evaluation strategy.....	27
3.2.2.2.2. IPIL calculation when using a simultaneous test and evaluation strategy .....	28
3.2.2.3. Results .....	30
3.3. Discussion.....	31
3.4. Conclusion.....	32

Chapter 4 - A NEW EVALUATION STRATEGY USING SUB-BAND ANALYSIS FOR DEALING WITH IMPULSE NOISE FROM SMALL FIREARMS .....	33
4.1. Introduction .....	33
4.2. Methods.....	34
4.2.1. OBIPIL concept .....	34
4.2.2. A BC correction approach for estimating IPIL and ANE.....	35
4.2.3. Design principles of the OB filter bank.....	39
4.3. Results .....	44
4.3.1. Results when the HPD is the Combat Arms Earplugs Gen IV with OPEN vents.....	44
4.3.2. Results when the HPD is the Combat Arms Earplugs Gen IV with CLOSED vents.....	45
4.3.3. Results when the HPD is the Superfit 30 Earplug .....	46
4.3.4. Results when the HPD is the X5A ear muff .....	47
4.3.5. Results when the HPD is the X5A ear muff combined with the Combat Arm earplugs with open vents	48
4.3.6. Results when the HPD is the X5A ear muff combined with the Combat Arm earplugs with closed vents.....	49
4.3.7. Results when the HPD is the X5A ear muff combined with the Superfit 30 earplugs.....	50
4.4. Discussion.....	51
4.5. Conclusion.....	53
Chapter 5 - GENERAL DISCUSSION .....	54
Chapter 6 - GENERAL CONCLUSION .....	58
REFERENCES.....	59
ANNEX A – Time and frequency domain performances of the OB Filter Bank .....	63
ANNEX B – Statistical methods and data presentation .....	69
ANNEX C – Experimental results and calculations.....	70
ANNEX D – CAF hearing conservation requirements when using a 5.56 mm caliber firearm .....	77

# List of Figures

Figure 1: T&E evolution from the Development tests to the Operational tests .....	5
Figure 2: Range of Human Hearing between 20Hz and 20 KHz .....	8
Figure 3 : Schematic of the human ear (from commons.wikimedia.org) .....	9
Figure 4 : Perspective and plan views of the ANSI/ASA impulse noise test setup [3] .....	15
Figure 5: Test Setup Building Effort - Top view .....	16
Figure 6 : Test Setup Building Effort - 1m contour .....	17
Figure 7: Sound radiations measurement for a small firearm .....	17
Figure 8: Sensor Grid for small arms radiations measurements .....	18
Figure 9: Sensor used to measure the exposure level .....	19
Figure 10: PPL radiations measurements at 1, 2, 4 and 8 meters from the small firearm .....	20
Figure 11 : Matlab routine estimating the 140 dB location at each radiation axis. ....	22
Figure 12 : Matlab routine estimating the 140 dB location at each radiation axis. ....	23
Figure 13: 140 dB Contour plot .....	23
Figure 14: GRAS 45CB Acoustic Test Fixture (ATF) .....	24
Figure 15: Impulse Noise Test Setup - Principle .....	25
Figure 16 : Impulse Noise Test Setup - Implementation .....	25
Figure 17: Unoccluded ear for an Anatomical human ear model.....	26
Figure 18: Occluded ear for an Anatomical human ear model .....	26
Figure 19: IPIL calculation when using a sequential test and evaluation strategy .....	28
Figure 20: IPIL by using simultaneous measurements.....	29
Figure 21: OBIPILSubband(dB) calculation steps.....	35
Figure 22 : OBIPIL versus BC limits for the 3M X5A earmuff and the 3M X5A combined with a 3M Combat Arms earplugs with open vents .....	36
Figure 23 : OBIPIL BC Corrected when combining the 3M X5A earmuffs and the 3M Combat Arms (Open vents) earplugs.....	36
Figure 24: OBIPILBC Corrected(dB) calculation approach .....	38
Figure 25: OBIPIL versus BC limits for the 3M Combat Arms earplugs with open vents .....	44
Figure 26: OBIPIL versus BC limits for the 3M Combat Arms earplugs with closed vents .....	45
Figure 27: OBIPIL versus BC limits for the Superfit 30 earplug.....	46
Figure 28: OBIPIL versus BC limits for the Superfit 33 earplug.....	47
Figure 29: OBIPIL versus BC limits for the Combat Arms earplugs with open vents & X5A earmuffs when used together for double protection.....	48
Figure 30: OBIPIL versus BC limits for the Combat Arms earplugs with closed vents & X5A earmuffs when used together for double protection.....	49
Figure 31: OBIPIL versus BC limits for the Superfit 30 earplugs with closed vents & X5A earmuffs when used together for double protection.....	50
Figure 32 : IPIL versus IPIL BC Corrected for the tested HPDs .....	51
Figure 33 : ANE when BC corrected for the tested HPDs.....	52
Figure 34: Acoustic spectral magnitude distribution at the MO location when the SA is fitted with and without a suppressor .....	56

# List of Tables

Table 1: HPDs Test Scenarios.....	15
Table 2: Radiation Axis and Angle matching table.....	18
Table 3: Experimental PPL measurements and decay calculations.....	21
Table 4 : Experimental location of the 140 dB contour.....	22
Table 5: Measurements and trials sequence for each test scenario .....	27
Table 6: IPIL and ANE measurements when using different T&E strategies .....	30
Table 7: BC attenuation limits (in dB) as per ANSI/ASA S12.42-2010 .....	35
Table 8 : Measured versus estimated HPD performances .....	44
Table 9: Measured versus estimated HPD performances .....	45
Table 10: Measured versus estimated HPD performances .....	46
Table 11: Measured versus estimated HPD performances .....	47
Table 12: Measured versus estimated HPD performances .....	48
Table 13: Measured versus estimated HPD performances .....	49
Table 14: Measured versus estimated HPD performances .....	50
Table 15 : Limitations and future work .....	54

# List of Acronyms

AHAAH	Auditory Hazard Assessment Algorithm for Human
ANE	Allowed Number of Exposure
ATF	Acoustic Test Fixture
CAF	Canadian Armed Forces
dBA	Decibels A weighted, re 20 microPascals (20 $\mu$ Pa)
dB	Decibels, re 20 microPascals (20 $\mu$ Pa)
dBp	Decibel unweighted peak, re 20 microPascals (20 $\mu$ Pa)
DND	Department of National Defence
DRC	Damage Risk Criteria
EEM	Equal Energy Model
HPD	Hearing Protection Device
IHC	Inner Hair Cells
IPIL	Impulse Peak Insertion Loss
MO	Military Operator
NIHL	Noise Induced Hearing Loss
OBIPIL	Octave Band Impulse Peak Insertion Loss
OEM	Original Equipment Manufacturer
OHC	Outer Hair Cells
PPL	Peak Pressure Level (in dB SPL)
RTO/NATO	Research and Technology Organization / North Atlantic Treaty Organization
SEL	Sound Exposure Level
SPL	Sound Pressure Level
TFOE	Transfer Function of the Open Ear

# Chapter 1 – INTRODUCTION

## 1.1. Motivation and Previous work

MO (Military Operators) exposed to hazardous steady-state or impulsive noise levels in training must wear the most appropriate Hearing Protection Device (HPD) as required by the Canadian Armed Forces (CAF) general safety program [16], the CAF Operational Training Procedures [26], and the Canadian Occupational Health and Safety Regulations [27].

However, a report produced in 2004 by DRDC-Toronto [1], showing an escalating cost of claims for Noise Induced Hearing Loss (NIHL) in the CAF, supports the need to review and upgrade current hearing conservation practices. In fact in a Military environment, Military Operators (MOs) are exposed to a large number of impulse noise events, such as those experienced during the firing of small firearms and large caliber weapons, and which can vary greatly in terms of level, temporal and spectral characteristics. The energy from most impulse noise events is normally concentrated within just a few milliseconds and can be sufficiently high to produce auditory impairment to an unprotected ear.

The current noise regulations and standards are most suitable for the prevention of Noise Induced Hearing Loss (NIHL) when a human subject is exposed to steady state noises [34]. However, for the military, the work environment can often be characterized by high level impulsive noise such as the firing of weapons [35].

Since the current metrics for hearing damage risk criteria are developed based on steady state noises, the applicability of the risk criteria to high level impulse noises is limited, hence there is a need to develop a new set of risk criteria for high level impulse noises [36; 37]. Therefore, there exists a need to characterize the performance of HPDs under high level impulse noises generated by small firearms weapons [2; 38].

The primary mechanism of these protection devices is through attenuation. The attenuation properties of these HPDs are normally measured by the manufacturer according to existing standards using fixed-frequency steady state noises. However, the manufacturer doesn't provide any information about the attenuation performance of these HPDs under high level impulse noises, and hence, the level of protection offered under high level impulse noise is unknown [2; 39].

To assess the health risks for people exposed to impulsive noise, a commonly accepted approach is to measure the instantaneous peak sound pressure level ( $L_{pk}$ ) which is also defined as the Peak Pressure Level (PPL). However, the peak sound pressure level is just one of the several parameters that contributes to noise hazard; in reality the hazard is characterized not only by its peak pressure but also by its time history and spectral content [40].

## 1.2.Objectives and Organization

Whereas this research study does not evaluate damage risk criteria, the reduction of the PPL and the filtering of the noise spectrum are inherent characteristic of the HPD that need a careful review, taking into account:

- The physical limitations related to the technologies used for the test experiment;
- The physiological limitations related to the propagation of sound via the human body.

The present methods used to characterize the HPDs assume that the human subject is exposed to a steady state noise. Unfortunately, the measured performances of these protection systems under a steady state noise could not be used to predict the noise level inside the ear when dealing with impulse noise. On the other hand, since materials do have a nonlinear sound absorption performance [41], then it is obvious that the materials used for building the HPDs will not provide the same absorption performances when the system is exposed to different impulse noise levels [23], which is the case when using different small firearms types. Then, it is necessary to characterize the HPDs under a wide range of impulsive noises generated by small firearms.

In the case of this study, the HPDs will be tested under impulse noise sound emitted by a 5.56 mm caliber small firearm type and emitting a peak noise level between 155 to 165 dBP.

The measurement of the Impulse Peak Insertion Loss (IPIL) of these protecting devices is performed in accordance with the instructions set out in ANSI/ASA S12.42 [3]. However, the efficiency of the measured HPD performances is physiologically limited; in fact, sound attenuation via the HPDs is competing against the Bone Conduction (BC) pathways of sound [8; 59].

Because of these limitations, even when the sound transmitted to the ear canal is completely attenuated by the HPD, the sound reaching the cochlea via the BC transmission pathways can bypass the HPD and can still be loud enough to cause hearing damage [8; 59].

The objectives of this thesis are:

- Reviewing the test method used by ANSI/ASA [3], and investigating a possible test alternative increasing the reliability of the experimental measurements.
- Proposing a metric to gauge the HPDs performances.
- Proposing a calculation model estimating the Allowed Number of Exposures (ANE) to impulse noise, by taking into account the physiological limitations of the human body.

To achieve these objectives, this thesis is organized as follows:

Chapter 2 reviews the scope of the performance requirements used so far in the industry, trying to relate the HPD performance requirements with the operational effectiveness and safety needed for the user.

Chapter 3 reviews the standard HPDs testing strategies and investigates the level of their applicability when the impulse noise is a small firearm.

Chapter 4 reviews the standard HPD evaluation strategies and introduces the Octave Band Impulse Peak Insertion Loss (OBIPIL) as a metric to gauge the HPDs performances in the time-frequency domain against the BC limits. A correction approach is proposed to adjust the IPIL measured with an ATF to account for the BC limits.

Chapter 5 provides general discussion, the thesis conclusion and some suggestions for possible future improvements.

Annex A gives some of the most important performance results for the used Octave Band Filter Bank used in this thesis

Annex B gives the statistical formulas to analyse experimental data in this thesis, and shows how the statistical data is presented in this thesis

Annex C gives the experimental results and the most important calculations results

Annex D gives the CAF hearing conservation requirements when using a 5.56mm caliber firearm [62]. To meet these Canadian regulations on a military base, these mentioned requirements were strictly applied when performing the test trials for this R&D project

### **1.3. Contributions**

This thesis is proposing the following contributions:

- An amendment for the ANSI/ASA S12.42 -2010 Test & Evaluation procedures, to address the test case when firing with small firearms.
- A metric to gauge the performances of HPDs in the time-frequency domain.
- An amendment to the EEM with respect to the BC limits, to realistically estimate the ANEs, when shooting with small firearms.

## **Chapter 2 – SCOPE REVIEW OF THE HEARING PROTECTION DEVICES PERFORMANCE REQUIREMENTS**

Military Operators (MOs) are exposed to a broad range of impulse noise that can vary greatly in terms of level, temporal and spectral characteristics. The accurate characterization of the damaging noise is required, to mitigate the hearing damage risk for the MOs working under such conditions. In fact, it has been demonstrated that mechanical damage, as well as metabolic disturbances induced by intense sound exposure, lead to Noise Induced Hearing Loss (NIHL) (Saunders et al., 1985).

A Systems Engineering based Test and Evaluation (T&E) approach has been used, to review the goals of the known HPDs qualification T&E procedures. Hence, this chapter reviews the physiological boundaries of the human hearing system and the signal processing via the hearing sensory system, with the aim to define the technical specifications and the performance measurements to be verified to finally relate the HPD performances with the operational effectiveness and safety needed for the user.

Pros and cons of the proposed methodologies will be discussed.

### **2.1. The systems engineering approach**

Systems Engineering (SE) based Test and Evaluation (T&E) develops plans and methodologies to reduce or to eliminate the technical risks [13; 14], and it provides information to:

- Decision makers responsible for making the investment decision to procure/build a new system.
- Operational users to support the development of effective tactics, doctrines, and procedures.

As a system undergoes design and development, the emphasis in testing evolves gradually from Development Test & Evaluation (DT&E) to Operational Test & Evaluation (OT&E), where DT&E is about assessing detailed technical specifications and some specific performance measurements, and OT&E is about questions related to operational effectiveness and suitability.

The relationship between DT&E and OT&E is described by the following Fig.1.

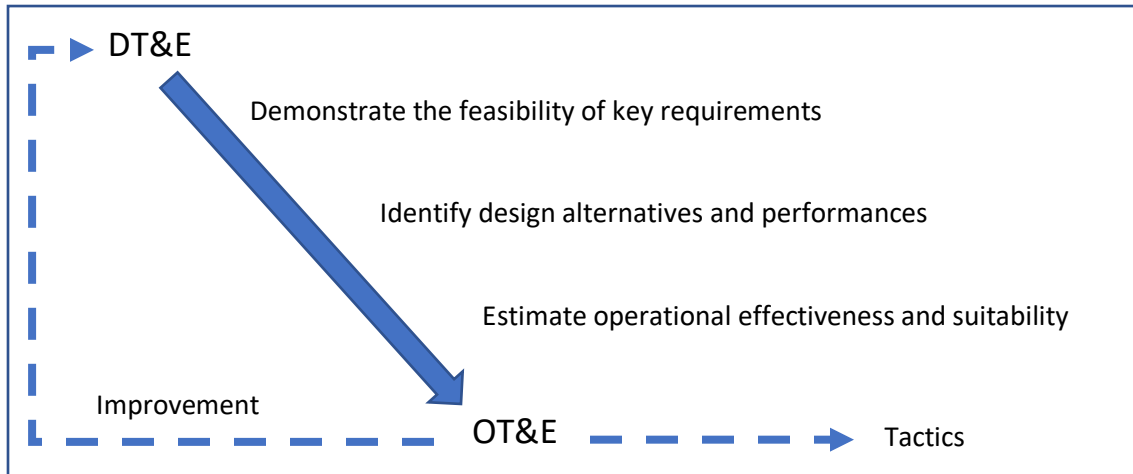


*Figure 1: T&E evolution from the Development tests to the Operational tests*

DT&E is focused on meeting detailed technical specifications, and generally it is based on existing standards [14].

The OT&E methodology for HPD characterisation considers the actual functioning of the equipment in realistic operational environment, in which the equipment must interact with men and peripheral equipment [14].

DT&E provides a view of the potential to reach technical objectives, and OT&E provides an assessment of the system's potential to satisfy the user requirements [14]. However, for continuous improvements, the outcome of the OT&E study impacts the DT&E by defining new specific performance requirements and goals, as illustrated in Fig.1.

## 2.2. Perception of sound

### 2.2.1 Frequency Scale:

The human ears are sensitive to relative variation in frequency of stimulus, which more generally means that an increase by a certain percentage in the frequency of stimulus is mandatory to be perceived as a constant pitch change in perception [56]. Consequently, for human hearing a frequency of stimulus  $R$  must be increased by a certain percentage to be perceived as a constant perceived change in pitch. More generally, the increment of a perceived quantity  $\Delta E$  is proportional to the ratio of the absolute increase of the physical property of the stimulus  $\Delta R$  and the physical property of the stimulus  $R$ . Therefore, the law of relative variation described by eq.1. applies:

$$\Delta E = k \frac{\Delta R}{R} \quad (1)$$

Where:

$E$  is the perceived quantity which is the pitch in this case;

$R$  is the stimulus which is the frequency in this case ;

$k$  is a constant of proportionality.

Doubling the frequency of the stimulus results in a constant or equal perceived pitch increase. As per eq.1, this could be translated as follows:

$$R + \Delta R = 2R \quad , \text{ then: } \frac{\Delta R}{R} = 1 \quad (2)$$

Since  $\Delta E$  from eq.1 is the pitch change, and by considering the result shown in eq.2, then for each doubling of the frequency:

$$\Delta Pitch = \Delta E = k \quad (3),$$

or:

$$Pitch + \Delta Pitch = E + \Delta E = E + k \quad (4).$$

which corresponds to a constant or equal pitch increase. This underlies the musical scale [57] indicating how the human ear works with respect to frequency, and that the subdivision of the frequency scale into octaves is based on doubling in frequency as per the following eq.5:

$$f_{n+1} = 2 \times f_n \quad (5)$$

Where:

$f_n$  : is the frequency at the centre of a specific bandwidth # $n$

$f_{n+1}$  : is the frequency at the centre of a specific bandwidth # $n+1$ .

Thus, using a logarithmic frequency scale displays each octave and approximates how the auditory system perceives sound frequencies.

Octave Bands (OBs) [48] represent a frequency scale approximating the human ear behavior. The Nominal mid-band frequencies of the OB scale in the audible range are: 31.5 Hz, 63 Hz, 125 Hz, 250 Hz, 500 Hz, 1000 Hz, 2000 Hz, 4000 Hz, 8000 Hz, 16000 Hz.

### 2.2.2 Intensity Scale:

The human ear perceives sounds higher than a certain minimal stimulus threshold  $R_0$  [56], representing a minimal sound pressure. In fact, humans are able to perceive sound pressures in the range of  $20 \cdot 10^{-6} N/m^2$  to approximately  $200 N/m^2$ , where the upper limit represents the pain threshold.

As per eq.1, this could be translated as follows:

$$dE = k \frac{dR}{R} \quad (6)$$

Integration yields:

$$E = k \ln\left(\frac{R}{R_0}\right) \quad (7).$$

This means that the human ear responds not linearly but logarithmically to sound loudness, thus it has been more practical to express acoustic measurements of loudness in a logarithmic scale.

Technically it is more practical to use a logarithmic scale for the sound pressure. Thus, the Sound Pressure Level (SPL) is defined as:

$$SPL = 20 \times \log_{10}\left(\frac{p}{p_0}\right) \quad (8)$$

Where:

$p$  : is the measured sound pressure over time

$p_0$ : is the reference sound pressure equal to  $20 \cdot 10^{-6} N/m^2$

### 2.2.3 Hearing Thresholds:

For a healthy person, the following diagram, Fig.2, provides the human threshold of audibility [55], and shows the audible limits of the Sound Pressure Level (SPL) and frequency.

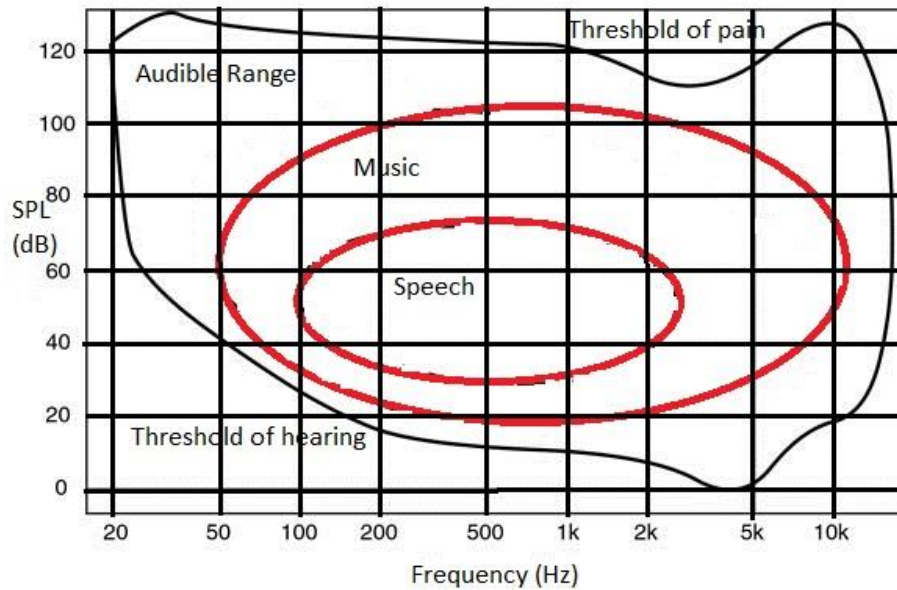


Figure 2: Range of Human Hearing between 20Hz and 20 KHz

### 2.3. Impulse noise as a health hazard

To analyse the impact of impulse noise on the hearing system it is necessary to understand the anatomy and physiology of the human ear, to clarify how the ear receives sound and transmits the information to the brain for decoding [9; 10; 11].

Several Damage Risk Criteria (DRCs) of impulse noise have been developed to prevent hearing damage when the human ear is exposed to damaging sound levels.

The U.S. Army developed the Auditory Hazard Assessment Algorithm for Human (AHA AH) software [48; 51; 52], based on a human ear circuit model designed to predict auditory hazard from blast exposures higher than 140 dBp, hence reducing the risk of Noise Induced Hearing Loss (NIHL). AHA AH models the physiological processes underlying hearing loss and then finds a measure that predicts it [50; 51]. In fact, in AHA AH the sound is processed in the human ear via three consecutive stages: the outer ear, the middle ear and the inner ear (Fig.3) and it does not consider all pathways of noise transmission (e.g. BC and other tissues).

# Anatomy of the Ear

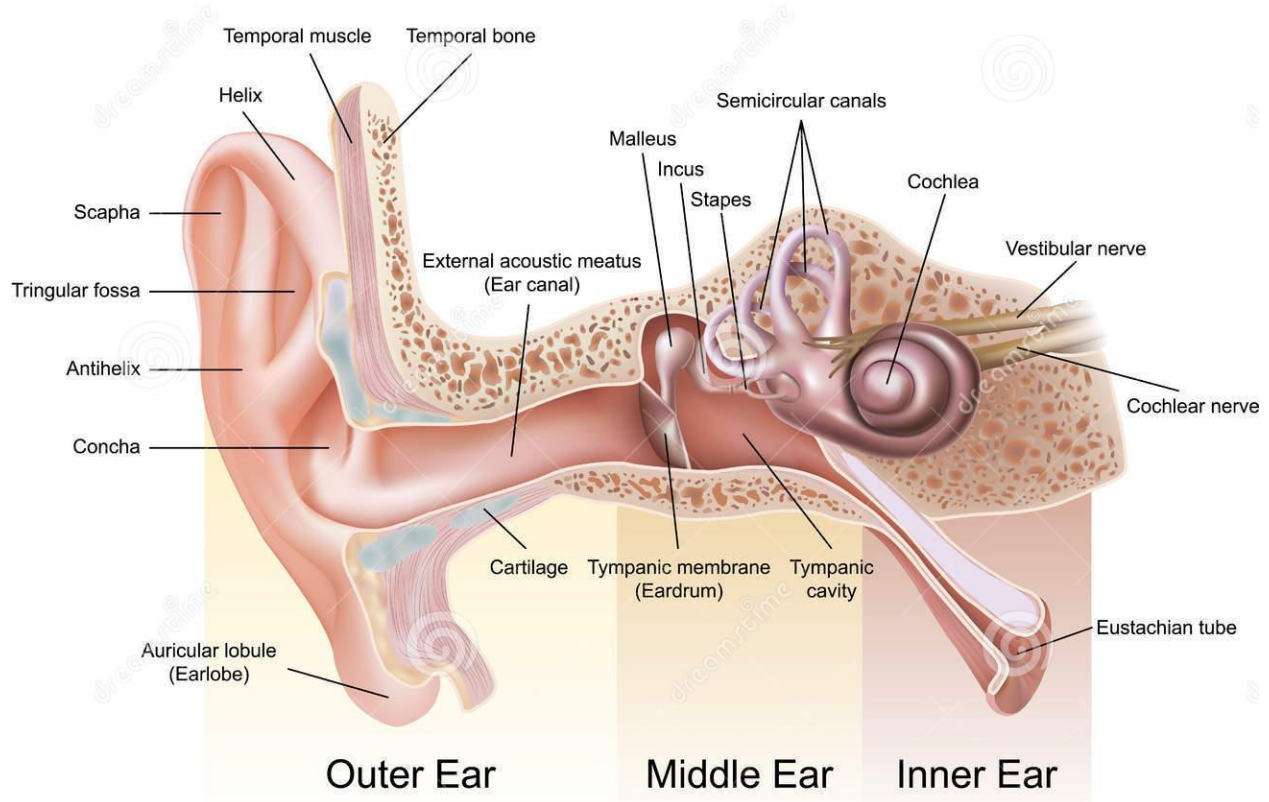


Figure 3 : Schematic of the human ear (from commons.wikimedia.org)

**The outer ear** is a sound guide, it receives the acoustic waves and concentrates the sound signal into the ear canal. The ear canal is about 2.5 cm and has one end open and one end closed, thus standing waves resonance [47;53] will occur at

$$f_n = \frac{n \cdot v}{4 \cdot L} ; n = 1,3,5,7 \quad (8)$$

Where:

$n$ , represents the harmonic number;

$v$ , represents the speed of sound 343 m/s;

$L$ , represents the ear canal length.

Because the outer ear increases the human ear sensitivity around the resonant frequency, and because the impulse noise is very rich in high frequencies, then the NIHL for MOs usually demonstrates a loss around the 4000 Hz frequency, and it also affects all the higher frequencies above 1 KHz, used for intelligibility and speech recognition [60;61].

The ear is very sensitive in the high frequency range between 2 KHz and 8 KHz; however the ear sensitivity doesn't depend only on frequency but also depends on sound intensity [54].

*The Middle ear* is a cavity section containing three small bones, and it transforms the acoustic signal into mechanical displacements and amplifies the sound intensity. When exposed to strong sound, the stapedius muscle contracts as a reflex, and it exerts some amplitude compression by reducing the input to the cochlea for sounds above 85 dB. However, since the acoustic middle ear reflex is relatively slow, the resulting amplitude compression affects steady and slowly varying sounds more than transient sounds as per impulse noise [9;10;11].

Therefore, as the impulse noise generated by a small firearm is such an intense and abrupt sound pressure wave, in the middle ear the eardrum membrane is likely to rupture, causing a temporary loss of hearing and a hazard infection of the middle ear. However, if no infection follows the injury, the membrane will heal [9;10;11].

*The Inner ear* is a spiral shape filled with fluid that analyzes the frequency content and the intensity of the waves. The amplitude compression that occurs in the cochlea allows a larger range of sound intensities to be coded in the auditory nerve. The amplitude compression in the cochlea is partly a result of the active role of Outer Hair Cells (OHC) and partly a result of the transduction process in Inner Hair Cells (IHC) [9; 10; 11].

Therefore, the impulse noise generated by a small firearm is such an intense and abrupt sound pressure wave that the OHCs may be damaged when exposed to an acoustic over-pressure [58]. Given that OHCs are in charge of the function of frequency selectivity in the basilar membrane within the cochlea and that the mammalian hair cells do not regenerate [12], then the loss of cells determines a permanent loss of the function of hearing frequency selectivity.

## **2.4. Methods used for HPD evaluation under impulse noise**

So far, the two main objective methods evaluating the HPD attenuation capabilities when dealing with impulse noise are the Acoustic Test Fixture (ATF) and the microphone in real ear (MIRE) [6; 7]. MIRE measurements only account for sound travelling through the ear canal and does not consider all pathways of noise transmission, as the missing pathways are the BC pathways [4; 5]. In addition, MIRE measurements are possible only if the sound doesn't induce a risk to the human subject used within the test loop, and that's why MIRE is not commonly used to evaluate HPDs for impulse noise [6].

The ATF method uses an adjustable mannequin to fit all ear sizes [3], where the ATF has a microphone built right into the ear canal. It also accounts only for sound travelling through the ear canal and does not consider all pathways of noise transmission (e.g. BC and other tissues) [3; 7; 8].

The metric used to evaluate the performance of HPDs uses an ATF, and it is called the Impulse Peak Insertion Loss (IPIL) [3]. It measures the difference, in the time domain, of peak pressure

values at the ATF ear microphone location, when the ATF ear is occluded and unoccluded. This measurement evaluates the capability of an HPD to attenuate the impulse noise level generated by a small firearm in the time domain.

## 2.5. Discussion

The sound intensity and the concentration of energy around some of the acoustic signal frequencies induce a destruction of some specific cochlear nerve cells, hence the occurrence of a permanent NIHL

So far:

- The methods used to characterize hearing protectors do not provide any information about the efficiency of the HPDs at the frequencies at which the ear become very fragile when exposed to high level impulse noise [2].
- The AHAAH software is subject to multiple controversies and limitations, the most obvious one being that this model has the limitation of not accounting for the Bone Conduction (BC) pathways [4].
- The Equal Energy Model (EEM) [18; 50] tried to correlate between some standard noise measurements and hearing loss [51]. It is built on the assumption that the risk of hearing loss produced by impulse noises will be monotonically increasing as the total A weighted energy received by experimental target increases [52]. However, most of the international standards recommend limiting the 8 hours exposure to less than 85 dBA.

The above overview of the physical performance of the human hearing system and review of the tools available to assess DRCs are defining the following goals for this research work, relating the HPD performances with the operational effectiveness and safety needed for the user:

Goal # 1: The performance measurements of hearing protectors, under impulse noise, must be performed over the frequency scale.

Goal #2: The performance measurements of hearing protectors, under impulse noise, must be performed in the logarithmic scale for loudness.

Goal #3: Propose a T&E method, taking into account the BC limits when estimating DRCs.

## 2.6. Conclusion

Impulse noise is a category of sound with a high Peak Pressure Level (PPL) in a very short time. It can permanently damage the OHCs and IHCs covering the surface of the basilar membrane and cause the detachment of the organ of Corti from the basilar membrane, hence a permanent damage can be produced over few noise pulses [48; 49].

To relate the HPD performances with the operational effectiveness and safety needed for the MO, it is necessary to use a time-frequency characterization approach to measure the performances of the HPDs.

An Acoustic Test Fixture (ATF) is to be used to support the OT&E efforts. The output of this Research and Development work should lead to impact the DT&E by defining new specific performance requirements, as illustrated in Fig.1.

## **Chapter 3 – REVIEW AND USE OF THE ANSI/ASA S12.42-2010 TESTING STRATEGY WHEN THE IMPULSE NOISE IS GENERATED BY A SMALL FIREARM**

Military Operators (MOs) are exposed to a broad range of impulse noise. An accurate test and evaluation of the performance of hearing protectors is required, to mitigate the hearing damage risk for the MOs working under such conditions. Presently, the accepted method to test Hearing Protection Devices (HPDs) performance is based on the measurement of the Impulse Peak Insertion Loss (IPIL), in dBP, according to the ANSI/ASA standard [3]. However, the mentioned standard doesn't provide enough information about the case where the radiated acoustic wave has a non-spherical acoustic propagation pattern, as per the case of small firearms. Therefore, in this chapter, two test and evaluation strategies are used to confirm that the asymmetry of the shock wave radiated by a small firearm and the inclusion of the MO in the test setup did not impact the measurement accuracy of the IPIL. Also, a sensor grid has been added to characterize the noise radiated from a 5.56 mm caliber small firearm arm.

In this Chapter 3:

- The testing procedure is reviewed for the case when small firearms are used;
- The required level of protection for the gunner and the crew members is provided;
- Two test and evaluation (T&E) strategies are compared, by using the IPIL criteria and the Allowed Number of Exposures (ANE) permitted for the MO, as per the equal energy model [18; 50].

Finally, pros and cons of the proposed methodologies will be discussed.

### **3.1. Introduction**

The Canadian Regulations stipulate that a safe exposure to noise levels must be, on average, no greater than 87 dBA over an eight-hour period [16; 24].

MO (Military Operators) in training exposed during 8 hours to an A-weighted sound pressure level of 87 dBA or greater, or Peak Pressure Level (PPL) of an impulse noise at or greater than 140 dBP, must wear an HPD as required by the CAF General Safety Program [16] and according to [25; 26; 27 and 29].

The performance of HPDs under impulse noise is measured according to ANSI/ASA S12.42 [3] using an Acoustic Test Fixture (ATF); this metric called IPIL accounts for HPD peak attenuation for a time domain signal.

The Safety protection criteria for protection against impulse noise, are as follows:

- (a) For an HPD, a minimum IPIL attenuation performance as defined by eq.9 is needed to ensure that the critical level from RTO/NATO is not exceeded for an impulse [18].

$$\min (IPIL) \geq SEL - 116 \text{ dBA} \quad (9)$$

Where 116 dBA is the critical Sound Exposure Level (SEL) limit in dBA for a single unprotected impulse, and SEL is the level of a constant sound lasting 1 sec that would contain the same amount of acoustical energy as the impulse [18], and measured at the MO location, Fig.9. The mathematical definition of SEL is as follows:

$$SEL = 10 \times \log_{10} \left( \frac{1}{T_0} \int_{-\infty}^{+\infty} \frac{p_A^2(t)}{p_0^2} dt \right) \quad (10)$$

Where,  $T_0$  is the reference duration of 1 sec,  $p_A(t)$  is the A-Weighted sound pressure in Pascals (Pa), and  $p_0$  is the reference sound pressure of  $20\mu Pa$  ( $2 \times 10^{-5} Pa$ ).

- (b) For MO exposed to impulse noise, and by setting the daily eight-hour equivalent energy limit to 87 dBA, the ANE [18] is calculated as follows:

$$ANE = 28800 \times 10^{-(SEL-IPIL-87)/10} \quad (11)$$

Where the IPIL represents the measurement obtained for a specific HPD, and the SEL is measured at the MO location, Fig.9.








- (c) For crew members exposed to impulse noise, the level of protection as per the American Hearing Conservation Program [25], must respect the following:
- When the PPL is less than 140 dBP, then an HPD may be worn;
  - When the PPL is from 140 to 165 dBP, then an HPD must be worn;
  - When PPL is greater than 165 dBP, then a combination of HPDs must be used.

#### *Hearing protection devices:*

Three HPDs manufactured by 3M were used for the experiment. Table 1 below lists the HPD configurations. Each HPD configuration is associated with a unique Test Scenario, leading for a total of seven test scenarios.

The HPDs used in this investigation are level dependent, which means that the device attenuation performances are sensitive to shifts of environmental sound PPLs, providing decreased attenuation performances with decreasing noise levels [23].

Table 1: HPDs Test Scenarios

Test Scenarios	Image
Combat Arms Gen IV earplugs with open vents	
Combat Arms Gen IV earplugs with closed vents	
Superfit 33 earplugs	
Peltor X5A earmuff	
Peltor X5A earmuff & Combat Arms Gen IV earplugs with open vents	
Peltor X5A earmuff & Combat Arms Gen IV earplugs with closed vents	
Peltor X5A earmuff & Superfit 33 earplugs	

### 3.2. Methods

MOs in training are exposed to hazardous impulsive noise levels occurring in reverberant and non-reverberant operational environments. Therefore, when the MO is exposed to a Peak Pressure Level (PPL) from a small firearm, then an adequate test procedure shall be used to measure the HPD performances under these operational conditions.

Because the acoustic wave is radiated in a non-spherical propagation pattern, it is necessary to measure the acoustic wave at different radiation axes to define the location after which using an HPD is mandatory.

So far, the performance of HPDs under impulse noise is measured according to the ANSI/ASA [3] standard. The test method presented in this standard uses a test setup where the probe, reference sensor, and the ATF are at the same distance from the noise explosion source, and both the ATF and the probe do have a relative angle, between their sagittal plane, equal to 30 degrees, Fig.4.

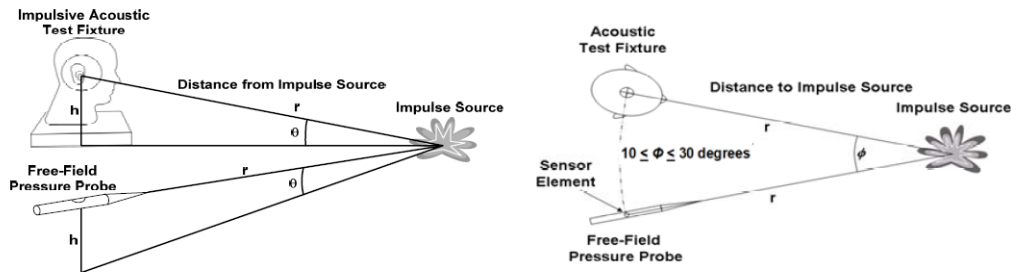


Figure 4 : Perspective and plan views of the ANSI/ASA impulse noise test setup [3]

This test setup configuration, Fig.4, assumes that the wave propagation from the explosion is spherical, which is not true when dealing with small firearms. In fact, the small firearms asymmetry results from the following factors:

- The main noise beam from the small firearm mouth is directed to the front;
- The small firearm ejection mechanism ejects the bullets on the right side of the weapon which adds additional high frequency components to the noise radiated on the right side of the small firearm comparing to the left side;
- The small firearm needs to be triggered by a human subject; then presence of the MO body interferes with the radiated acoustic waves especially at the back left side of the small firearm.

### 3.2.1. Characterisation of small firearm radiations

#### 3.2.1.1. Testing procedure

The measurements were performed at Canadian Forces Base Petawawa, on a clear day with an average temperature of 14 °C and average humidity of 27%. The average wind speed was 4 m/s (maximum 7 m/s) [17]. The shooting range was a fine grained soil open field with slits and clay.

A sensor grid has been used to perform the measurements. The grid covers multiple radiation axes. Some of the test setup pictures are shown in Fig.5, Fig.6 and Fig.7.

The sensors were positioned at the same height as the small firearm, and the angular increment from one radiation axis to the next one was fixed to 30° [17].



*Figure 5: Test Setup Building Effort - Top view*



*Figure 6 : Test Setup Building Effort - 1m contour*



*Figure 7: Sound radiations measurement for a small firearm*

The final sensor grid respects the geometrical dimension as presented by Fig.8.

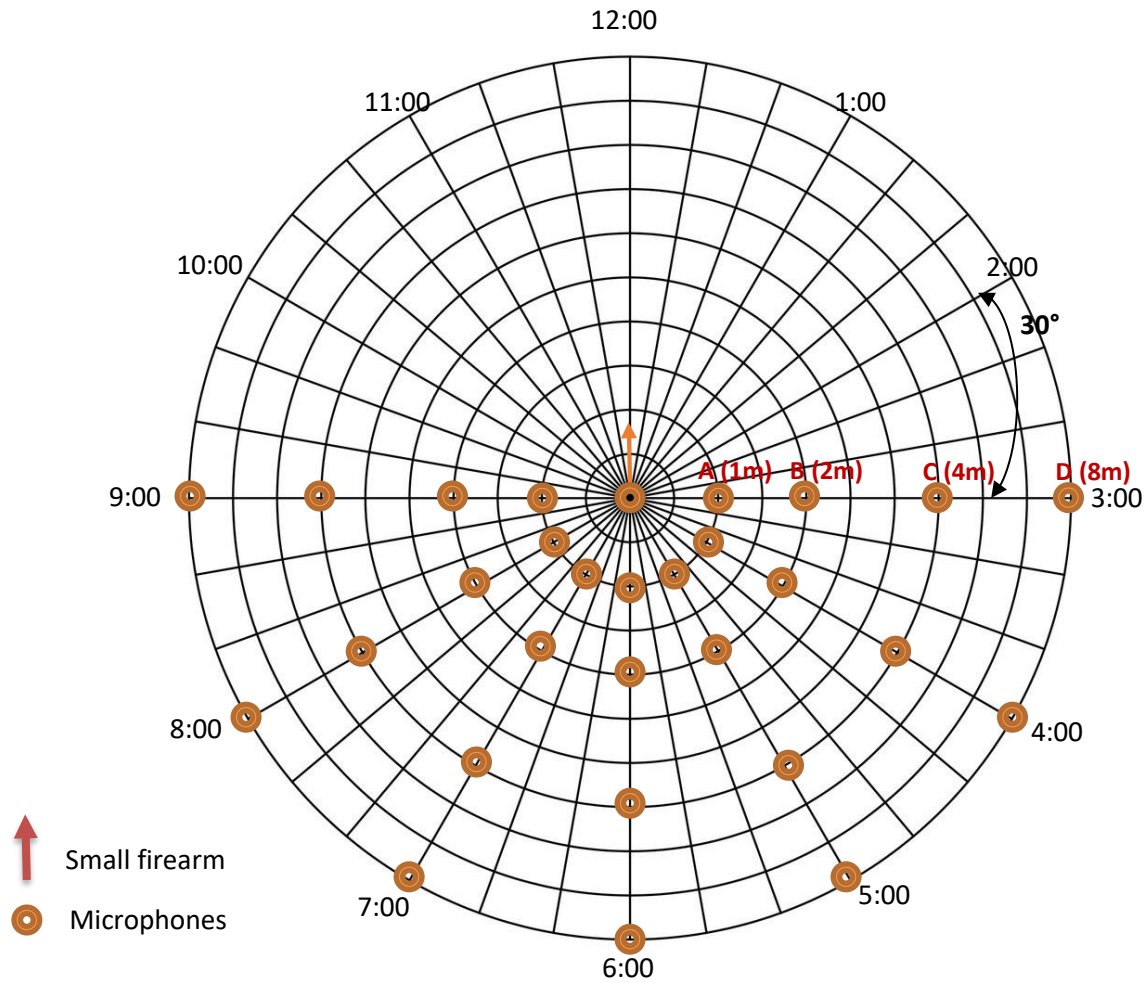


Figure 8: Sensor Grid for small arms radiations measurements

Since in this work we are interested in protecting the MO and the crew members, then the sound measurements were performed only between the 3:00-radiation axis and the 9:00-radiation axis.

In this work, the radiation axis is presented in the conventional time format. The following Table 2 shows the relationship between the radiation axis and its corresponding yaw angle.

Table 2: Radiation Axis and Angle matching table

Radiation Axis (hh:mm)	Yaw Angle (°)
3:00 (or 300)	0
4:00 (or 400)	30
5:00 (or 500)	60
6:00 (or 600)	90
7:00 (or 700)	120
8:00 (or 800)	150
9:00 (or 900)	180

Because of the acoustic wave asymmetry, relying on the sensor probe to measure the ATF or the MO exposure to impulse noise is not the right thing to do; therefore, the MO was instrumented with an acoustic sensor, Fig.9, to measure its exposure to impulse noise.



*Figure 9: sensor used to measure the exposure level*

Please note that:

- The sensor grid is built with a contour of sensors at 2m, 4m and 8m from the noise source, and covering the radiation axis from 3:00 to 9:00.
- The contour at 1m is named "A", the contour at 2m is named "B", the contour at 4m is named "C", and the contour at 8m is named "D".
- The MO location is defined to be at the center of the weapon, which is the location of the weapon cartridge.

### 3.2.1.2. Data Analysis & Results

The statistical methods and the data presentation format used in this section are described in Annex B, where the following format is used: Magnitude (Standard Deviation).

Measurements performed at the MO location at the small firearm stock, Fig.9, show that the PPL was equal to 156.7(0.6) dBp and the SEL was equal to 123.6 (0.7) dBA.

The PPL contour measurements performed by the sensor grid, Fig.8, are summarized by Fig.10.

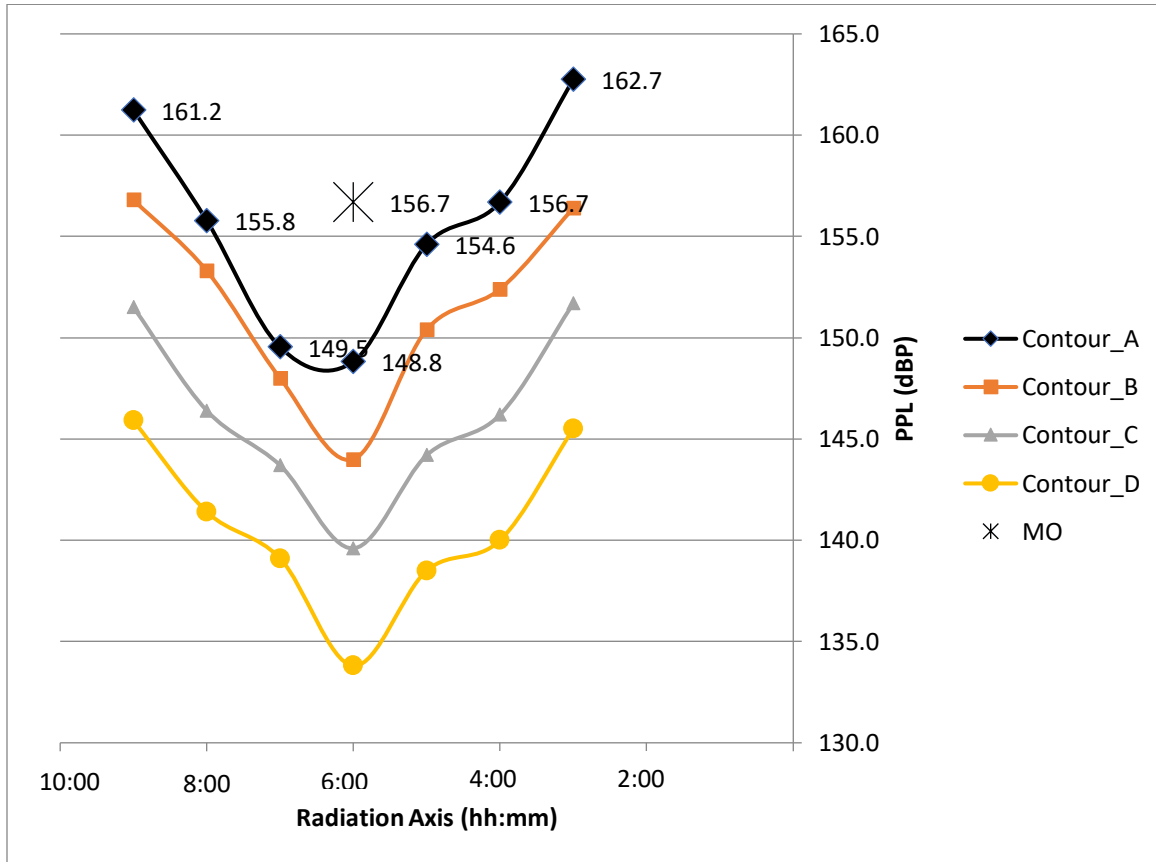


Figure 10: PPL radiations measurements at 1, 2, 4 and 8 meters from the small firearm

These results confirm that the radiated sound, when using a small firearm, has non-spherical propagation patterns. In fact, a pressure notch is observable at the MO location, Fig.10.

In free field, the sound pressure propagating follows eq.12 for two points located at the same radiation axis [19]:

$$PPL_1 - PPL_2 = 20 \times \log_{10} \left( \frac{r_2}{r_1} \right) \quad (12)$$

Where;  $PPL_1$  and  $PPL_2$  are the sound Peak Pressure Level at the distances  $r_1$  and  $r_2$ , in meters, from the radiating point source. Therefore, in free field the sound levels decay linearly by 6 dB when doubling the distance from a radiating point source. In the case of this test experiment, the experimental verification of the sound decay from contour A to contour B, from contour B to contour C and from contour C to contour D, Fig.8, is calculated as follows:

$$\begin{aligned} PPL_A - PPL_B &= Decay_{A-B} \\ PPL_B - PPL_C &= Decay_{B-C} \\ PPL_C - PPL_D &= Decay_{C-D} \end{aligned} \quad (13)$$

The experimental measurements and decay calculations are presented in the following Table 3.

*Table 3: Experimental PPL measurements and decay calculations*

Radiation Axis	Contour	PPL( $\sigma$ )	$Decay_{A-B}$	$Decay_{B-C}$	$Decay_{C-D}$
3:00	A	165.7(0.3)	6.3	4.7	6.2
	B	156.4(0.6)			
	C	151.7(0.2)			
	D	145.5(0.4)			
4:00	A	159.7(0.4)	4.3	6.2	6.2
	B	152.4(0.4)			
	C	146.2(0.4)			
	D	140(0.6)			
5:00	A	157.6(0.5)	4.2	6.2	5.7
	B	150.4(0.9)			
	C	144.2(0.7)			
	D	138.5(0.5)			
6:00	A	151.8(0.6)	4.8	4.4	5.8
	B	144(0.3)			
	C	139.6(0.6)			
	D	133.8(0.5)			
7:00	A	154.0(0.3)	1.5	4.3	4.6
	B	148(0.4)			
	C	143.7(0.5)			
	D	139.1(4.6)			
8:00	A	158.8(0.3)	2.5	6.9	5.0
	B	153.3(0.4)			
	C	146.4(0.2)			
	D	141.4(0.4)			
9:00	A	164.2(0.2)	4.4	5.3	5.6
	B	156.8(0.4)			
	C	151.5(0.4)			
	D	145.9(0.6)			

The results show that the measured decay was not always quasi-equal ( $\approx$ ) to 6dB. In fact, ground reflections, the influence of the atmospheric conditions and the presence of some obstacles as per the MO body influence the propagation of sound. Consequently, the attenuation does not decay linearly by 6 dB per doubling of distance from the source point.

In this case, the determination of the safety zone or the 140 dB contour [17], must be purely based on the experimental measurements, and could not be estimated by using the classical acoustic equation for free field.

To locate the 140dB distance from the radiating point source, a recursive calculation approach has been implemented, using a 1-D data interpolation Matlab function (interp1) with a linear interpolation method, with an extrapolation capability.

The following Matlab code lines, Fig.11, are showing the routine used to estimate the experimental location of the 140 dB level at each radiation axis:

```
% PPL2m is the Peak Pressure Level at 2m
% PPL4m is the Peak Pressure Level at 4m
% PPL8m is the Peak Pressure Level at 8m
radius = 2;
dB140 = 200;
while dB140 > 140
radius = radius + 0.05 ;
dB140 = interp1([2,4,8],[PPL2m,PPL4m,PPL8m],radius,'linear','extrap');
end
```

*Figure 11 : Matlab routine estimating the 140 dBP location at each radiation axis.*

The results generated by this calculation technique are presented in Table 4.

*Table 4 : Experimental location of the 140 dB contour*

Radiation Axis	9:00	8:00	7:00	6:00	5:00	4:00	3:00
140 dB location (m)	12.15	9.1	7.25	3.8	6.95	8.05	11.6

To link all the 140dB locations, with the aim to plot the 140 dB contour, a 1-D data interpolation Matlab function (interp1) with a linear interpolation method has been used. The following Matlab lines, Fig.12, show the calculation routine:

```

% polar plot
theta = [ 180 , 180+30 , 180+60 , 270 , 270+30 , 270+60 , 360 ] ;
Cont_140db = [ 12.15 , 9.1 , 7.25 , 3.8 , 6.95 , 8.05 , 11.6];
j=1;
for i=180:360
    Cont_140db_interp(j)=interp1(theta,Cont_140db, i, 'linear');
    angle(j)=i;
    j=j+1;
end
figure
p = polarplot(deg2rad(angle),Cont_140db_interp,'blue')
rlim([0 15])
title('140 dB Contour')
legend([p], '140dB', 'Location', 'southwest', 'Orientation', 'horizontal')

```

*Figure 12 : Matlab routine estimating the 140 dBP location at each radiation axis.*

Hence, the 140 dB contour plot is presented by Fig.13.

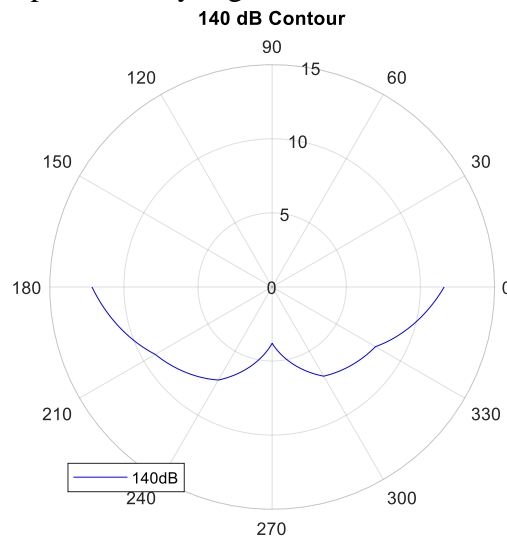


*Figure 13: 140 dB Contour plot*

### 3.2.2. Characterization of Hearing Protection Devices

Characterizing HPDs under impulse noise is critical to guarantee the hearing safety of the MO, In fact, knowing the ANEs is necessary to protect MOs when training. The equal energy principle [18; 50] proposes a formula estimating the ANE limit based on the IPIL of the HPD system and the SEL encountered by the MO.

In the previous section 3.2.1, a tuned test setup has been investigated to cover for the case when the radiated acoustic wave is non-spherical. In this section, a sequential T&E method is proposed to confirm the validity of the ANSI/ASA calculation method when firing with small firearms, and to open the way to a more robust T&E strategy that could be very handy when dealing with reverberant like environments.

#### 3.2.2.1. Testing procedure

The measurements were performed at Canadian Forces Base Connaught, on a clear day with an average temperature of 9 °C and average humidity of 63%. The average wind speed was 3 m/s (maximum 7 m/s) [17]. The shooting range was a fine grained soil open field with slits and clay.

The measurements were performed using a 45CB ATF, Fig.14, and a 46DD-FV microphone, Fig.16, (G.R.A.S. Sound & Vibration, Holte, Denmark). The ear canals of the ATF were heated to 37°C before the measurements. Data were acquired with a sixteen-channel Siemens LMS system running PLM Software at a sampling rate of 204.8 kHz. The data acquisition recordings are in accordance with the requirements of [3]; for each impulse event the left and right ATF and free-field pressure probe signals are recorded simultaneously.



*Figure 14: GRAS 45CB Acoustic Test Fixture (ATF)*

To generate the impulse noise, an MO was integrated into the ANSI/ASA S12.42 test scenario, as described by Fig.15 and Fig.16, and as recommended in section 3.2.1.3.

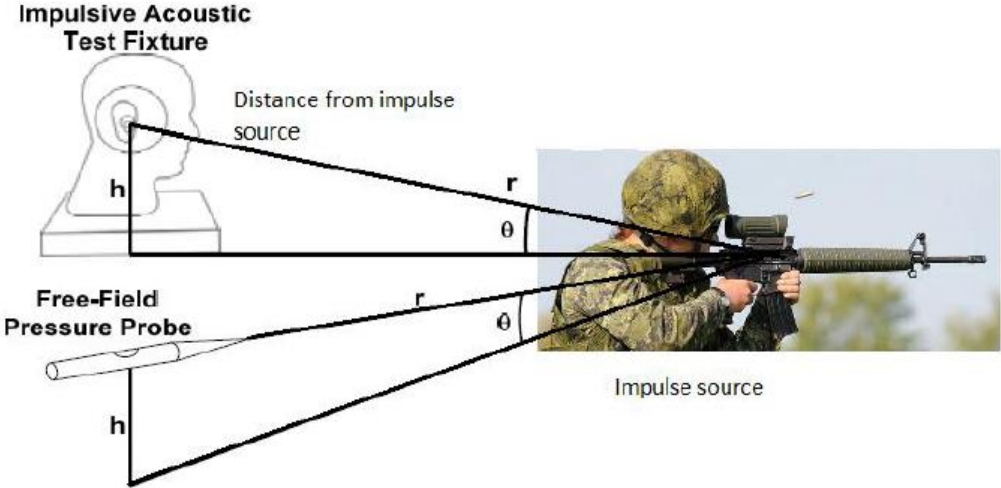


Figure 15: Impulse Noise Test Setup - Principle



Figure 16 : Impulse Noise Test Setup - Implementation

The sensors placement respected the following geometry:

- The ATF was positioned at a height of 1.7meters;
- The distance between the firing weapon and the ATF was 1 meter;
- The relative angle between the sagittal plane of the ATF and the pressure probe was equal to 30 degrees;
- The distance between the pressure probe and the ATF was equal to 0.52 m;
- The ATF was oriented directly facing the impulse noise source within  $\pm 3$  degrees;
- The impulse noise source was a 5.56 mm caliber small firearm, producing a PPL of 156.7(0.6) dBP and an SEL of 123.6(0.7) at the arm stock.

The selected ATF has anthropometrically representative dimensions of the head and the hearing system. The left and right microphones inside the ATF measure the noise levels at the ear drum location of each ear.

Measurements for each test scenario involve repeated measurement of the ATF open-ear Signals (unoccluded), Fig.17, followed by repeated measurement of the ATF closed-ear signals (occluded), Fig.18, for each HPD sample.



*Figure 17: Unoccluded ear for an Anatomical human ear model*



*Figure 18: Occluded ear for an Anatomical human ear model*

The HPD is removed and refitted between the two conditions. Table 5 details the measurement sequences for each test scenario.

*Table 5: Measurements and trials sequence for each test scenario*

a	ATF <b>Unoccluded</b> measurement	Five bullets are fired
b	Fitting HPDs into the ATF	
c	Waiting period of 120s	
d	ATF <b>Occluded</b> measurement ( <b>Trial 1</b> )	Five bullets are fired
e	Removing HPD from the ATF	
f	For the second trial ( <b>Trial 2</b> ), repeat the sequence: (b),(c),(d),(e)	

### 3.2.2.2. Data analysis

Two test and evaluation strategies estimating the IPIL when fitting an ATF with an HPD are presented and discussed in the following sub-sections (3.2.2.2.1) and (3.2.2.2.2).

The first T&E strategy has been designed to avoid using TFOE when estimating the IPIL, and the second one presents the standard T&E strategy used by ANSI/ASA.

#### 3.2.2.2.1. IPIL calculation when using a sequential test and evaluation strategy

By definition, the IPIL is the PPL difference when the ears of the ATF are occluded and unoccluded. Therefore, it is the measurement of the pressure peak attenuation in the time domain raw data and is calculated by using the difference of the pressure peak pressure values of  $P_{ATF_{Unoccluded}}(t)$  and  $P_{ATF_{Occluded}}(t)$  [3].

When expressed in the time domain, the IPIL equation is formulated as follows:

$$IPIL(Pa) = P_{k-ATF_{Unoccluded}} - P_{k-ATF_{Occluded}} \quad (14)$$

Where,  $P_{k-ATF_{Unoccluded}}$  is the peak pressure measurement when the ATF is unoccluded and  $P_{k-ATF_{Occluded}}$  is the PPL measurement when the ATF is occluded.

By using the same approach to express the difference in dB, the definition of IPIL in decibels would be as follows:

$$IPIL(dB) = 20 \times \log_{10} \left( \frac{P_{k-ATF_{Unoccluded}}}{P_0} \right) - 20 \times \log_{10} \left( \frac{P_{k-ATF_{Occluded}}}{P_0} \right) \quad (15)$$

Where,  $P_0$  is the reference sound pressure of  $20\mu Pa$  ( $2 \times 10^{-5} Pa$ ).

Therefore:

$$IPIL(dB) = PPL_{ATF_{Unoccluded}} - PPL_{ATF_{Occluded}} \quad (16)$$

Where,  $PPL_{ATF_{Unoccluded}}$  is the Peak Pressure Level when the ATF is unoccluded, and  $PPL_{ATF_{Occluded}}$  is the Peak Pressure Level when the ATF is occluded.

This test and evaluation strategy is summarized in Fig.19. The IPIL measurement is obtained by sequentially measuring the unoccluded ATF ear response, Fig.17, and then placing the HPD on the ATF and measuring the occluded ATF response, Fig.18. Subtracting the second peak value from the first peak value leads to the IPIL.

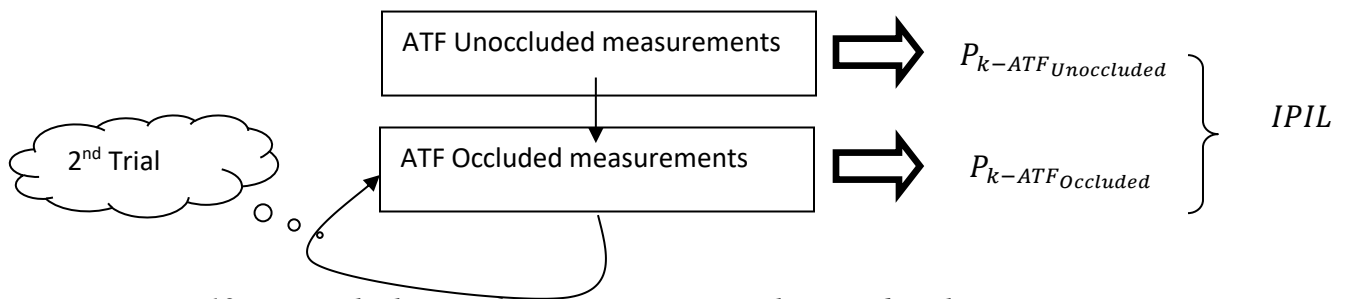


Figure 19: IPIL calculation when using a sequential test and evaluation strategy

However, this sequential test and evaluation approach, Fig.19, assumes that the source signal was identical for all the measurements, which is not true in practice.

In fact, with small firearms as impulse noise sources, there are likely to be small variations in the signals between trials, particularly in an outdoor environment and because the energy contained in bullets from the same caliber is not identical, even when the ammo is from the same cartridge.

### 3.2.2.2.2. IPIL calculation when using a simultaneous test and evaluation strategy

The following IPIL calculation approach is described by the ANSI/ASA [3] standard; it uses the unoccluded measurement to determine the Transfer Function of the Open Ear (TFOE), by assuming that the TFOE doesn't change between measurements for a given source and measurement configuration.

The TFOE or  $H_{ff}$  is a function of frequency (f) defined as

$$H_{ff}(f) = \frac{F(P_{ATF_{Unoccluded}}(t))}{F(P_{FF}(t))} \quad (17)$$

Where,  $F$  is the Fourier transform and  $P_{ATF\_Unoccluded}$  and  $P_{FF}$  are the pressure time signals measured at the ATF ear drum and free field probe, respectively. The transfer function  $H_{ff}$  is averaged over the number of repetitions.

The occluded measurements are used to measure the occluded signal inside the ATF ear drum  $P_{ATFOccluded}(t)$  and the free field signal  $P_{FF}(t)$  is the measurement at the reference probe. Therefore both TFOE and  $P_{FF}$  are used to estimate the unoccluded ear signal  $P_{Est-ATFUnoccluded}(t)$  at the ATF ear drum.

Therefore, the IPIL expression in the time domain is as follows:

$$IPIL(Pa) = P_{k-Est-ATFUnoccluded} - P_{k-ATFOccluded} \quad (18)$$

With:

$$P_{k-Est-ATFUnoccluded} = \max \left[ F^{-1} [H_{ff}(f) \times F(P_{FF}(f))] \right] \quad (19)$$

Where:

$P_{k-Est-ATFUnoccluded}$  is the estimated unoccluded peak pressure when the ATF is occluded;

$P_{k-ATFOccluded}$  is the measured peak pressure when the ATF is occluded.

This test and evaluation strategy is summarized in the following Fig.20. The IPIL measurement is obtained by simultaneously measuring the unoccluded ATF ear response, as in Fig.17, and the occluded ATF response, as in Fig.18. Subtracting the second peak value from the first estimated peak value leads to IPIL.

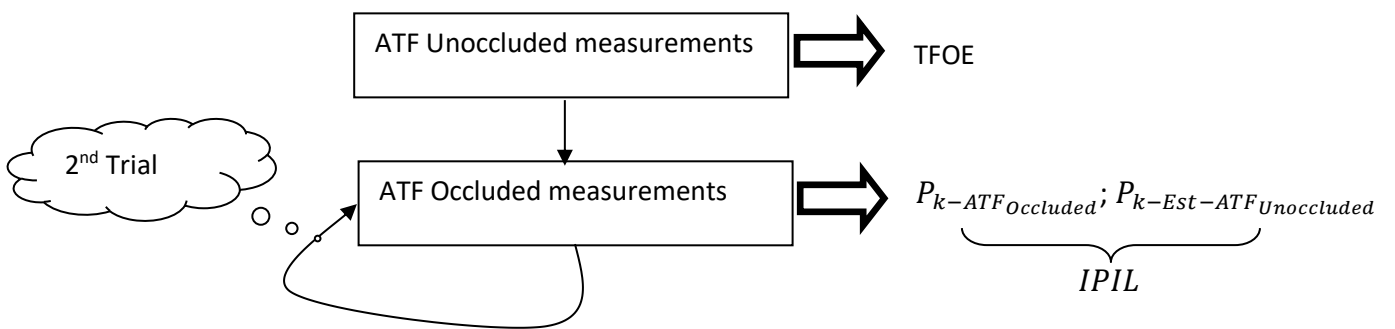


Figure 20: IPIL by using simultaneous measurements

However, this simultaneous test and evaluation approach, shown in Fig.20, assumes that the TFOE is the same for all the measurements, which will require further validation and R&D work to confirm the linearity of the TFOE when the PPL varies by +/- 3 dB.

### 3.2.2.3. Results

The measurements that were made are shown in Annex B, while some analysis of the results is presented below. The calculation of the ANE depends on the SEL, the IPIL and the daily eight-hour equivalent energy limit of 87 dBA, as stated in eq.11.

Considering the need to compensate for the measurements standard deviation and accounting for possible minimal losses because of fitting issues encountered by trained personnel, a realistic protection should be 3 dB below the measured IPIL [21; 22], which means that a realistic ANE must be cut by 50%.

$$ANE_{realistic} = ANE/2 \quad (20).$$

The estimated IPIL and ANE values and their corresponding standard deviation ( $\sigma$ ) are presented in the following Table 6. The SEL used for this calculation is measured at the MO location and is equal to 123.6 (0.7) dBA. Table 6 is providing the final IPIL and ANE calculations for different T&E strategies.

Table 6: IPIL and ANE measurements when using different T&E strategies

Test Scenario		Sequential T&E strategy		Simultaneous T&E strategy	
HPD System	Image	IPIL ( $\sigma$ 1)	$ANE_{realistic}$	IPIL ( $\sigma$ 2)	$ANE_{realistic}$
3M – Combat Arms Earplugs Gen IV (OPEN vents)		32.7 (1.8)	5825	32 (1.7)	4999
3M – Combat Arms Earplugs Gen IV (CLOSED vents)		47.8 (3.2)	187.828	47.7 (3.3)	187.265
3M, Superfit 33		46.9 (2.1)	153.017	45.8 (2.2)	120.504
3M – X5A		37.8 (2.3)	19.125	38.1 (2.2)	20.344
3M – X5A & Combat Arms (OPEN vents)		44.1 (1.7)	80.716	45.0 (1.3)	98.581
3M – X5A & Combat Arms (CLOSED vents)		52.2 (2.1)	526.990	53 (1)	631.552
3M – X5A & Superfit 30		58.1(1.9)	2.037.080	59.9(3.3)	3.076.305

The results show that:

- The two IPIL calculation methods are providing comparable results;
- The highest IPIL value was achieved by using a double protection with closed vents and the lowest value was obtained with an open vent earplug.

### 3.3. Discussion

#### (A) Characterisation of small firearm radiations:

- Non-spherical acoustic wave propagation:

Test results presented in Fig.10 and Fig.13 confirm that the acoustic wave is radiated in a non-spherical acoustic propagation pattern. The asymmetry of the shock wave radiated by a small firearm and the participation of an MO should not significantly impact the measurement accuracy of the IPIL, since these values are computed from a differential calculation.

Therefore, the usage of the Transfer Function of the Open Ear (TFOE), eq.17, to estimate the IPIL as described by the ANSI/ASA [3] when shooting with a small firearm, could demonstrate some measurement accuracy issues because the multiple reflections from the ground and from the MO could potentially impact the phase between the signals measured at the probe and at the ATF.

- Safety zone for MO and crew members:

The 140 dBp contour shown in Fig.13 defines the space zone where the crew members must use HPDs. Here it is assumed that crew members are located only in the space between the 3:00-radiation axis and the 9:00-radiation axis, as shown by Fig.8.

Measurements performed at the MO location, Fig.9, show that the operator was exposed to a PPL of 156.7(0.6) dBp. Since the PPL is below 165 dBp, the MO doesn't need double protection to protect his ears [25]. However, using double protection will increase safety and increase the ANEs when firing with a small firearm.

- Sensors location:

In this test experiment, level dependent and nonlinear HPDs are used. Hence to get the right IPIL estimation for the MO it is recommended to test these systems at the same PPL level as that encountered at the MO location. However, practically it was difficult to implement the test setup, Fig.15, because of the geometric (space) limitations.

Based on the test results shown in Fig.10, locating the ATF at the 5:30 radiation axis and the sensor probe at the 6:30 radiation axis, and at 1 m from the center of the small firearm:

- Meets the ANSI/ASA test setup geometrical requirements;
- Exposes the ATF and the Pressure probe to very similar PPLs, because of the bilateral symmetry of the radiated acoustic wave;

- Exposes the HPDs to a PPL range within 6dB (Table 3) of the PPL measured at the MO location. At this location, the HPDs are assumed to show similar attenuation characteristics to those obtained if the measurement was performed at the MO location.

## **(B) Characterization of Hearing Protection Devices:**

By taking into account that the IPIL is the result of a differential calculation, then it becomes clear that the influence of the sound propagation issues, discussed in 3.2 and 3.2.1.3.A, disappear.

The results presented in Table 6 show that the IPIL calculations for both the sequential and the simultaneous T&E strategies are providing very comparable results. This confirms that the proposed sequential T&E strategy is a robust method that leads to the same results as the simultaneous one presented by ANSI/ASA [3].

The calculation of the IPIL using the sequential T&E strategy doesn't require the estimation of the TFOE. Consequently, the sequential T&E strategy, compared to the simultaneous one, has the advantage of providing reliable test results without using the reference probe, which reduces a lot the complexity of the test setup, especially when the space allocated to the test is limited.

The robustness of the sequential T&E strategy should be confirmed in a reverberant test environment, where the multiple sound reflections should affect the magnitude measurement at each sensor and the phase between the different sensors.

## **3.4. Conclusion**

In this chapter, a revisit of the ANSI/ASA [3] test procedure was performed in the context where the noise source is a small firearm.

Section 3.2.1 focused on the measurement of the noise signature on multiple radiation axes, and then proposed some refinements to the test setup, initially proposed by ANSI/ASA [3], to increase the reliability of the measurements when the impulse noise is generated by a small firearm.

Section 3.2.2 compared between two different IPIL T&E strategies. Both alternatives have provided reliable and comparable results in the context where a MO is used to generate the impulse noise via a small firearm. Therefore, the ANSI/ASA[3] calculation method estimating the IPIL value is still valid when firing with a small firearm. However, introducing the sequential T&E approach has potential for IPIL measurements validation, especially when the test environment is inducing multiple sound reflection paths (e.g. reverberant test environment).

## **Chapter 4 - A NEW EVALUATION STRATEGY USING SUB-BAND ANALYSIS FOR DEALING WITH IMPULSE NOISE FROM SMALL FIREARMS**

Military Operators (MOs) are exposed to a broad range of impulse noise that can vary greatly in terms of level, temporal and spectral characteristics. The accurate characterization of the performance of hearing protectors is required, to mitigate the hearing damage risk for the MOs working under such conditions. Presently, the accepted method to characterize Hearing Protection Devices (HPDs) performance is based on the measurement of the Impulse Peak Insertion Loss (IPIL). However, this measurement doesn't provide the peak Insertion Loss (IL) per Octave Band (OB). A method for measuring the peak IL per OB for HPDs is developed and presented in this chapter. The concept of an Octave Band Impulse Peak Insertion Loss (OBIPIL) is introduced to account for the HPD peak attenuation at each OB. Using a modified version of the ANSI/ASA S12.42-2010 test setup, the impulse noise signals for a 5.56 mm caliber weapon were recorded. The IPIL and the OBIPIL values of the tested HPDs were computed and are presented for comparison. Moreover, an OBIPIL comparison versus the Bone Conduction (BC) attenuation limits is provided to gauge the attenuation capabilities of each HPD at each OB. A performance behavior for each HPD is presented in the time domain and per OB. Also, a BC based correction approach is proposed to adjust the IPIL measured with an ATF, to the limitations imposed by the human auditory system. Finally, remarks, conclusions, pros and cons of the proposed methodology as well as future work are discussed.

### **4.1. Introduction**

The Canadian Standards Association (CSA) rates HPDs as Class A, B, or C. This method defines the minimum attenuation at different OBs [24]. Other rating systems include the Noise Reduction Rating [30] and the Single Number Rating [31], in decibels, which serve the purpose of providing a single value to describe the effectiveness of an HPD. None of these rating systems are valid for impulse noise. The performance of HPDs under impulse noise is measured according to ANSI/ASA S12.42 [3] using an Acoustic Test Fixture (ATF); this metric is called the impulse peak insertion loss (IPIL) and accounts for HPD peak attenuation for a time domain signal.

The measurements used in this chapter were performed and detailed in the previous chapter. However this part of the work introduces the concept of Octave Band Impulse Peak Insertion Loss (OBIPIL), with the purpose of accounting for HPD peak attenuation at each OB. Therefore, comparing the peak attenuation with the Bone Conduction (BC) attenuation at each OB becomes possible, and a BC based correction to the IPIL is also proposed.

## 4.2. Methods

The IPIL measurement in the time domain does not provide any information about the acoustic impulse attenuation capabilities at each OB of the HPD system [32], nor does it provide enough information to compare the HPD attenuation capabilities against the BC attenuation over the OB spectrum. Hence, decomposing the raw time domain signal into time-frequency domain signals at each OB is the key idea to measure the peak pressure at each OB, and then the IPIL attenuation at each OB is called OBIPIL in this thesis.

Because of its simplicity and its verified reliability, the sequential test and evaluation strategy presented in the previous chapter 3 is used to carry out the data analysis portion in this chapter.

### 4.2.1. OBIPIL concept

The IPIL measurement is formulated in the time domain as shown in eq.14. Therefore, when expressed in the time-frequency domain, the peak pressure variation at a specific sub-band is represented by  $OBIPIL_{Subband}$  and is now defined as follows:

$$OBIPIL_{Subband}(Pa) = (P_{k-ATF_{Unoccluded}})_{Subband} - (P_{k-ATF_{Occluded}})_{Subband} \quad (21)$$

By using the same approach to express the difference in dB, the definition of IPIL per OB in decibels is as follows:

$$OBIPIL_{Subband}(dB) = 20 \times \log_{10} \left( \frac{(P_{k-ATF_{Unoccluded}})_{Subband}}{P_0} \right) - 20 \times \log_{10} \left( \frac{(P_{k-ATF_{Occluded}})_{Subband}}{P_0} \right) \quad (22)$$

Where,  $(P_{k-ATF_{Unoccluded}})_{Subband}$  and  $(P_{k-ATF_{Occluded}})_{Subband}$  represent the peak pressure measurement at a sub-band level, when the ATF is unoccluded and occluded, respectively.

Consequently:

$$OBIPIL_{Subband}(dB) = (PPL_{ATF_{Unoccluded}})_{Subband} - (PPL_{ATF_{Occluded}})_{Subband} \quad (23)$$

Where,

$(PPL_{ATF_{Unoccluded}})_{Subband}$  is the PPL per sub-band when the ATF is unoccluded;

$(PPL_{ATF_{Occluded}})_{Subband}$  is the PPL per sub-band when the ATF is occluded;

$OBIPIL_{Subband}(dB)$  is the level of variation at a specific sub-band.

In this work the time-frequency signal decomposition is performed by using a non-uniform, perfect-reconstruction filter bank design based on an FFT and inspired from [33], which will be detailed in section 4.2.3.

The summary of the calculation steps to obtain the  $OBIPIL_{Subband}(dB)$ , are presented in Fig.21.

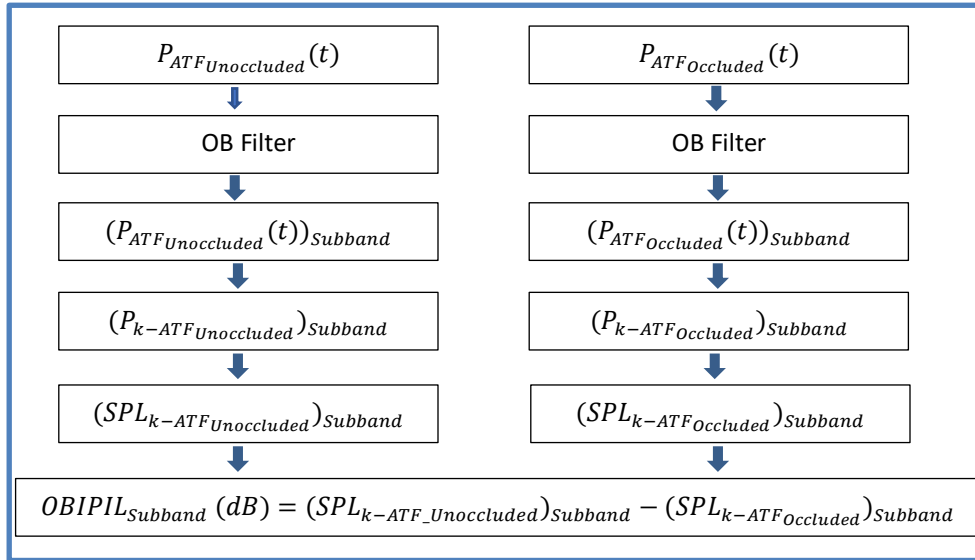


Figure 21:  $OBIPIL_{Subband}(dB)$  calculation steps

#### 4.2.2. A BC correction approach for estimating IPIL and ANE

The concept of a BC limits implies that the sound transmitted via the human skull bypasses the normal air-conduction pathways through the ear canal [5]. Consequently, even if the sound transmitted to the ear canal is completely attenuated by an HPD, the sound reaching the cochlea via the BC pathways is still loud enough to cause hearing damage [8].

Technically, the BC pathways limits the maximum attenuation that can be achieved generally with a double protection [8]. The BC attenuation limits (in dB) when the head is not covered [3; 5] are presented in the following table 7.

Table 7: BC attenuation limits (in dB) as per ANSI/ASA S12.42-2010

Frequency	125 Hz	250 Hz	500 Hz	1000 Hz	2000 Hz	4000 Hz	8000 Hz
BC limit (dB)	50	57	61	49	41	50	50

The OBIPIL metric provides the opportunity to compare BC amplitude attenuation limits against HPD amplitude attenuation limits, when the HPDs are used under impulse noise conditions. This comparison is necessary to gauge the provided protection level at some specific OBs, especially between 2 to 4 kHz where the human hearing system is known to be very sensitive. Fig.22 shows that for the specific case of the 3M X5A earmuff and the 3M combat arms earplug with open vents, the double protection is overprotecting when the frequencies are higher than 1 kHz.

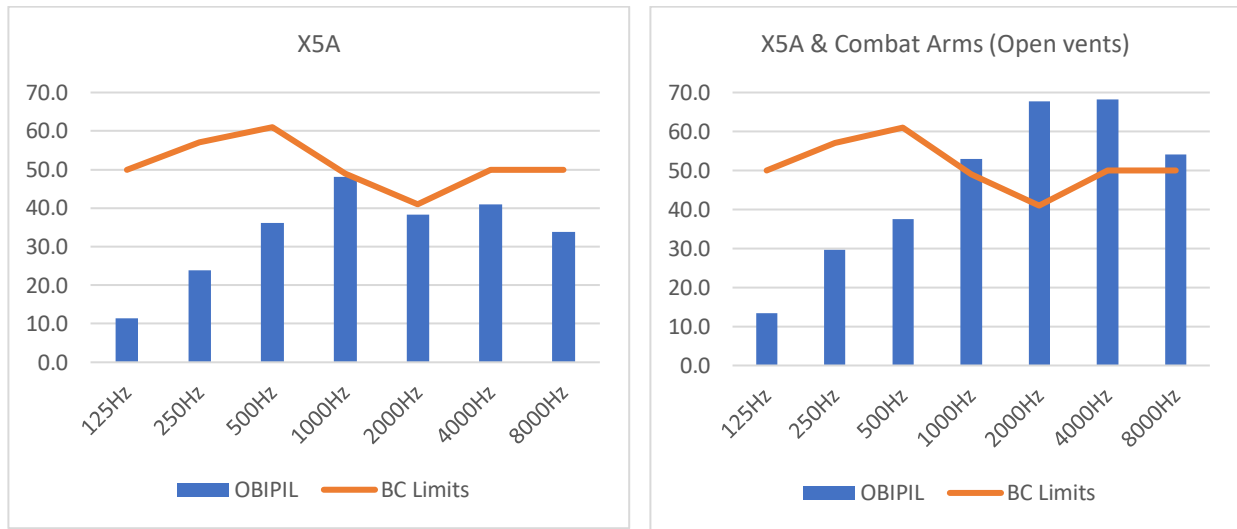


Figure 22 : OBIPIL versus BC limits for the 3M X5A earmuff and the 3M X5A combined with a 3M Combat Arms earplugs with open vents

However, the double protection is realistically having its OB attenuation capability capped at the BC limits, therefore the OBIPIL must be BC corrected, as shown by Fig23.

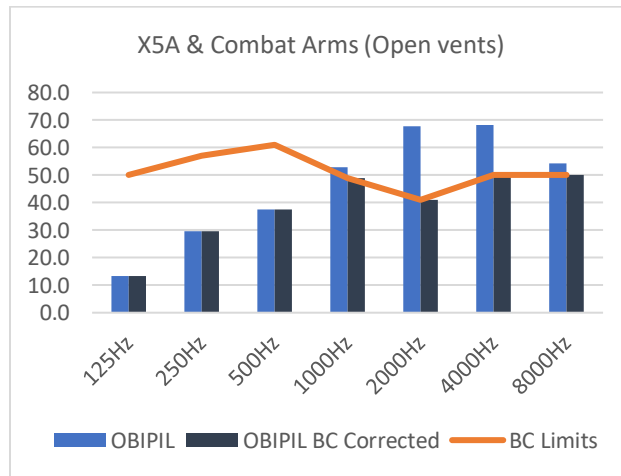


Figure 23 : OBIPIL BC Corrected when combining the 3M X5A earmuffs and the 3M Combat Arms (Open vents) earplugs

The OBIPIL BC corrected equation, would be written:

$$OBIPIL_{BC\ Corrected} (dB) = \min(OBIPIL, BC_{limits}) \quad (24)$$

By using the OBIPIL definition, eq.24, and by considering that an effective protection for the human ear must be BC corrected, then the  $OBIPIL_{BC\ Corrected} (dB)$  in the frequency domain would be written as follows:

$$OBIPIL_{BC\ Corrected} (dB) = (PPL_{ATF\_Unoccluded})_{Subband} - (PPL_{Est\ at\ Human\ Ear_{Occluded}})_{Subband} \quad (25)$$

Where,

$(PPL_{ATF\_Unoccluded})_{Subband}$  is the PPL per sub-band when the ATF is unoccluded;

$(PPL_{Est\ at\ Human\ Ear_{Occluded}})_{Subband}$  is the estimated PPL per sub-band when the human ear is occluded;

$OBIPIL_{BC\ Corrected} (dB)$  is the level of variation at a specific sub-band.

Therefore, the equation estimating the PPL per OB at the human ear is

$$OBIPIL_{BC\ Corrected} (dB) = (PPL_{ATF\_Unoccluded})_{Subband} - (PPL_{Est\ at\ Human\ Ear_{Occluded}})_{Subband} \quad (26)$$

Consequently, the PPL per OB estimated at the human ear would be:

$$(PPL_{Est\ at\ Human\ Ear_{Occluded}})_{Subband} = (PPL_{ATF\_Unoccluded})_{Subband} - OBIPIL_{BC\ Corrected} (dB) \quad (27)$$

By calculating the overall cumulative Sound Pressure Level (SPL), as given by eq.28, for the signals  $(PPL_{ATF\_Unoccluded})_{Subband}$  and  $(PPL_{Est\ at\ Human\ Ear_{Occluded}})_{Subband}$ :

$$SPL_{estimated} = 10 \times \log_{10} \left( \sum_{Subband=125\ Hz}^{8000\ Hz} 10^{\frac{PPL_{Subband}}{10}} \right) \quad (28)$$

it becomes possible to calculate the value of the BC corrected IPIL

$$IPIL_{BC\ Corrected} (dB) = (SPL_{ATF\_Unoccluded})_{estimated} - (SPL_{Est\ at\ Human\ Ear_{Occluded}})_{estimated} \quad (29)$$

Consequently, by taking into account eq.20, the effective BC corrected ANE calculation would be written as per the following eq.30.

$$ANE_{BC\ Corrected} = 0.5 * 28800 \times 10^{-(SEL_{MO} - IPIL_{BC\ Corrected} - 87)/10} \quad (30)$$

Where,

$SEL_{MO}$  : is the SEL measured at the MO location;

The summary of the calculation steps leading to obtain the effective ANE, is presented in the following Fig.24.

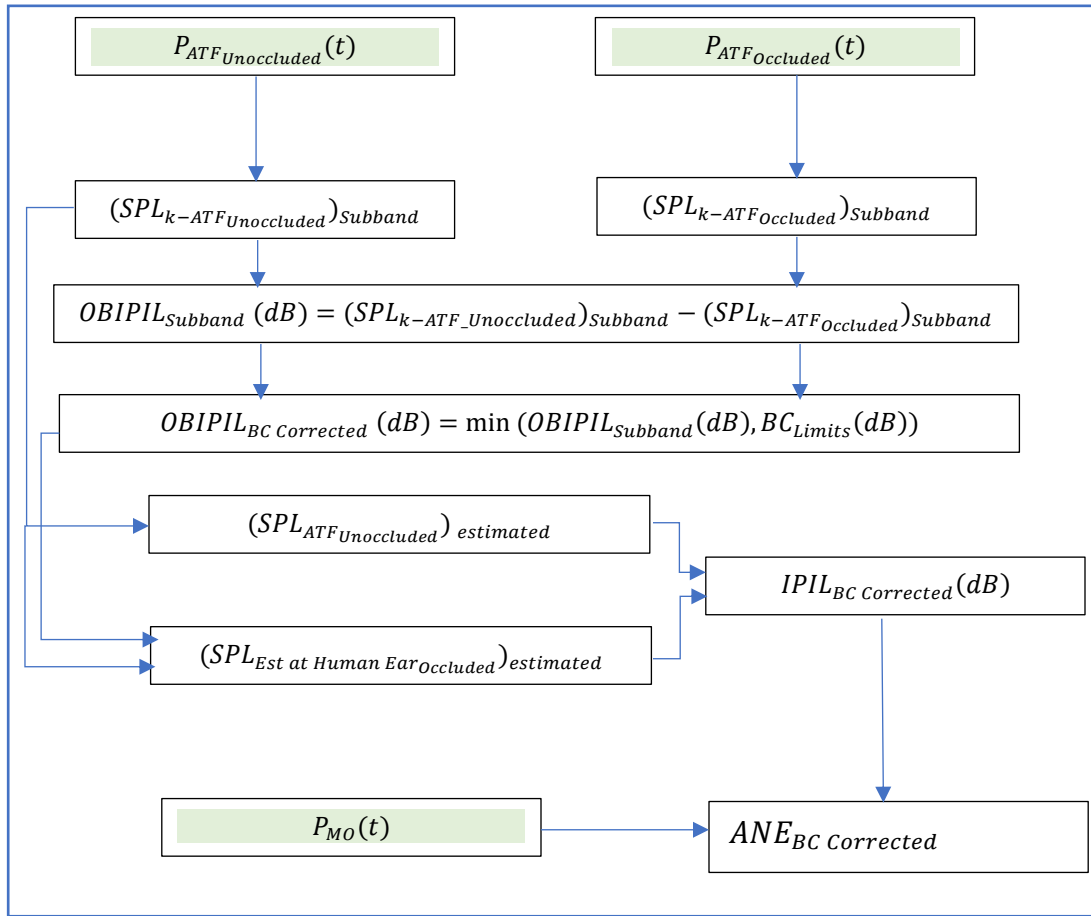


Figure 24:  $OBIPIL_{BC\ Corrected}(dB)$  calculation approach

### 4.2.3. Design principles of the OB filter bank

The design of the OB filter bank is based on the FFT-based method presented in [33], which is adapted below. The aim is to obtain bandpass filters with linear phase properties, leading to perfect reconstruction, based on simple FFT (without use of any optimization), and for arbitrary passbands (e.g. 1/3<sup>rd</sup> octave in our case).

Consider bandpass causal type-I (symmetric) linear phase FIR filters with real-valued coefficients and with the following form:

$$h_{sb}[n - (L-1)/2] ; 0 \leq n \leq L-1 \quad (31)$$

where  $L$  is the number of coefficients in each filter (odd value), and  $h_{sb}[n]$  corresponds to non-causal even symmetric filters with non-zero values over  $-\frac{L-1}{2} \leq n \leq \frac{L-1}{2}$ . The combination of those filters must result in a perfect reconstruction of an input signal  $x[n]$ , with a constant group delay of  $(L-1)/2$ :

$$y[n] = \sum_{sb} y_{sb}[n] = \sum_{sb} (h_{sb}[n - (L-1)/2] * x[n]) = x[n - (L-1)/2] \quad (32)$$

where  $y_{sb}[n]$  is the output of each filter,  $x[n]$  is the input signal, and “\*” denotes a linear convolution sum.

Having different bandpass responses for each  $h_{sb}[n - (L-1)/2]$  filter allows to perform a frequency decomposition of the input signal  $x[n]$ , in the different sub-band output  $y_{sb}[n]$  signals. Increasing  $L$  improves the frequency decomposition (improving the frequency selectiveness of the bandpass filters). However, the perfect reconstruction condition holds for any value of  $L$ .

Moreover, the FIR filters  $h_{sb}[n - (L-1)/2]$  are all linear phase, with the same constant group delay of  $(L-1)/2$  samples. This allows simple comparisons between the aligned real-valued time signals  $y_{sb}[n]$  at the output of each sub-band filter  $h_{sb}[n - (L-1)/2]$ , as well as a comparison with the delayed original input signal  $x[n - (L-1)/2]$  (which corresponds to the sum of all  $y_{sb}[n]$  signals).

The  $h_{sb}[n - (L-1)/2]$  filters can be considered like standard sub-band/filter bank analysis filters, although here we do not need the typical operations of downsampling, upsampling, and synthesis filtering normally performed in filter banks and sub-band processing.

Since  $x[n-(L-1)/2] = \delta[n-(L-1)/2] * x[n]$ , from the above equation we can write that the criteria for perfect reconstruction becomes:

$$\sum_{sb} h_{sb}[n-(L-1)/2] = \delta[n-(L-1)/2] ; 0 \leq n \leq L-1 \quad (33)$$

or

$$\sum_{sb} h_{sb}[n] = \delta[n] ; -(L-1)/2 \leq n \leq (L-1)/2 \quad (34)$$

Consider the time-wrapped (modulo- $N$ )  $0 \leq n \leq N-1$  versions of the above  $h_{sb}[n]$  and  $\delta[n]$  signals, with  $N=L$ . The case  $N > L$  works as well, but we use  $N=L$  in the derivation below for simplicity. The previous equality still holds after the modulo- $N$  operation:

$$\sum_{sb} h_{sb}[n\%N] = \delta[n\%N] = \delta[n] \quad 0 \leq n \leq N-1 \quad (\text{where “\%N” defines a modulo-}N \text{ operation}) \quad (35)$$

If we apply a  $N$ -point FFT to both sides, the condition becomes:

$$\sum_{sb} H_{sb}[k] = 1 \quad 0 \leq k \leq N-1. \quad (36)$$

Since  $N=L$  in this simplified derivation, we can also write:

$$\sum_{sb} h_{sb}[n\%L] = \delta[n\%L] = \delta[n] \quad 0 \leq n \leq L-1 \quad (37)$$

$$\sum_{sb} H_{sb}[k] = 1 \quad 0 \leq k \leq L-1. \quad (38)$$

This condition is very easy to achieve, for example using non-overlapping passband responses  $H_{sb}[k]$ , with real-valued unit gain in each passband and no gaps between passbands, i.e., rectangular bandpass responses in the  $k$  FFT frequency domain. Or, by using any combination of real-valued bandpass responses  $H_{sb}[k]$  that leads to real-valued unit gain when the responses are summed. To have real-valued filter coefficients in the time domain, the complex-conjugate symmetry condition in the FFT domain must be met  $H_{sb}[k] = H_{sb}^*[L-k]$   $1 \leq k \leq (L-1)/2$  (also an easy condition to meet). Finally, forcing each  $H_{sb}[k]$  to be real-valued will ensure that each corresponding time domain  $h_{sb}[n]$  is even-symmetric, and that  $h_{sb}[n-(L-1)/2]$  is a causal type I symmetric linear phase FIR filter.

For a given value of the number of coefficients  $L$ , it is possible (and recommended) to add a time domain window function to improve the frequency response/selectivity (e.g. reduced sidelobes from a sub-band leaking in other sub-bands). Consider the time-wrapped (modulo-  $L$  ) filters obtained from the IFFT of each bandpass response  $H_{sb}[k]$ , with odd  $L$  value:

$$h_{sb}[n\%L] = IDFT\{H_{sb}[k]\}; 0 \leq n \leq L-1. \quad (39)$$

For a given value of  $L$ , to reduce the stopband and passband ripples in the frequency response  $H_{sb}(e^{j\omega})$  of each  $h_{sb}[n - (L-1)/2] \quad 0 \leq n \leq L-1$  filter (and to reduce the redundancy between the different  $y_{sb}[n]$  output signals), a non-rectangular even-symmetric  $L$ -point window  $w[n] \quad -(L-1)/2 \leq n \leq (L-1)/2$  can be applied to each bandpass filter:

$$h_{sb}[n\%L] = h_{sb,i}[n\%L]w[n\%L] \quad 0 \leq n \leq L-1 \quad (40)$$

or equivalently

$$h_{sb}[n] = h_{sb,i}[n]w[n] \quad -\frac{L-1}{2} \leq n \leq \frac{L-1}{2} \quad (41)$$

where  $h_{sb,i}[n\%L]$  (with corresponding FFT response  $H_{sb,i}[k]$ ) represents a bandpass response before the application of the window function, and  $h_{sb}[n\%L]$  (with corresponding FFT response  $H_{sb}[k]$ ) is now considered to be a response after the application of the window.

To determine the effect of the windowing operation on the perfect reconstruction property, we have:

$$\sum_{sb} h_{sb}[n] = \delta[n] \quad -(L-1)/2 \leq n \leq (L-1)/2 \quad (\text{perfect reconstruction windowed responses}) \quad (42)$$

$$\sum_{sb} (h_{sb,i}[n]w[n]) = \delta[n] \quad -(L-1)/2 \leq n \leq (L-1)/2 \quad (43)$$

$$\sum_{sb} (h_{sb,i}[n]w[n]) = \delta[n] \quad -(L-1)/2 \leq n \leq (L-1)/2 \quad (44)$$

$$\left( \sum_{sb} h_{sb,i}[n] \right) w[n] = \delta[n] \quad -(L-1)/2 \leq n \leq (L-1)/2 \quad (45)$$

$$\left( \sum_{sb} h_{sb,i}[n\%L] \right) w[n\%L] = \delta[n\%L] = \delta[n] \quad 0 \leq n \leq L-1 \quad (46)$$

Because  $\sum_{sb} H_{sb,i}[k] = 1 \quad 0 \leq k \leq L-1$ , we also have that  $\sum_{sb} h_{sb,i}[n\%L] = \delta[n\%L] = \delta[n]$  over the considered range, so this reduces to:

$$\delta[n] w[n\%L] = \delta[n] \quad 0 \leq n \leq L-1 \quad (47)$$

which is true as long as:

$$w[0] = 1 \quad (48)$$

which is again a very easy condition to achieve, it only implies a scaling on any window function  $w[n]$  used.

The design steps are then:

1. Determine the value of  $L$  based on the desired passband to stopband transition width for the bandpass filters, as well as the level of ripple in each passband and stopband (also controlling the level of overlap/redundancy between filter outputs). Increasing  $L$  improves the frequency decomposition (ideal frequency selective filters), however the perfect reconstruction condition holds for any value of  $L$ .
2. Define the desired passbands (e.g. uniform bands or  $1/3^{\text{rd}}$  octave bands) using non-overlapping  $H_{sb,i}[k]$  responses with real-valued unit gain in each passband and zero gain elsewhere (automatically leading to  $\sum_{sb} H_{sb,i}[k] = 1$ ). Ensure that  $H_{sb}[k] = H_{sb}^*[L-k]$   $1 \leq k \leq (L-1)/2$ , to have real-valued time domain coefficients.
3. Compute  $h_{sb,i}[n\%L] = \text{IDFT}\{H_{sb,i}[k]\} \quad 0 \leq n \leq L-1$
4.  $h_{sb,i}[n-(L-1)/2] = h_{sb,i}[(n-(L-1)/2)\%L] \quad 0 \leq n \leq L-1$  (i.e.,  $h_{sb,i}[n\%L]$  shifted by  $(L-1)/2$ , then modulo  $L$  operation is applied)
5. Apply window:  $h_{sb}[n-(L-1)/2] = h_{sb,i}[n-(L-1)/2] w[n-(L-1)/2] \quad 0 \leq n \leq L-1$  (with  $w[0] = 1$ )

6. (optional) Verify the design by plotting the magnitude frequency responses of the causal type-I linear phase FIR filters  $h_{sb}[n-(L-1)/2]$   $0 \leq n \leq L-1$ , as well as by verifying the perfect reconstruction property. Note that if a unit sample is used as  $x[n]$  in order to measure the impulse response of each bandpass filter, then  $\delta[n-M]$   $M \geq (L-1)/2$  should be used in order to observe the full causal symmetric response in the sub-band filter responses  $h_{sb}[n-(L-1)/2]$   $0 \leq n \leq L-1$ .

The parameters used for the design of the filters in this work are:

- FFT size  $N = 2^{15} = 32768$
- Filter length (nb. coefficients)  $L=N-1 = 32767$
- Blackman window
- 9 octave bands, having the following center frequencies : 125 Hz; 250 Hz; 500 Hz; 1000 Hz; 2000 Hz; 4000 Hz; 8000 Hz; 16000 Hz; 32000 Hz.

Some results illustrating the characteristics of the filter bank are presented in Annex A.

### 4.3. Results

#### 4.3.1. Results when the HPD is the Combat Arms Earplugs Gen IV with OPEN vents

Results in Fig.25 shows that the tested HPD doesn't need to be BC corrected, and in fact the OBIPIL amplitudes did not exceed the BC limits for a non-covered head.

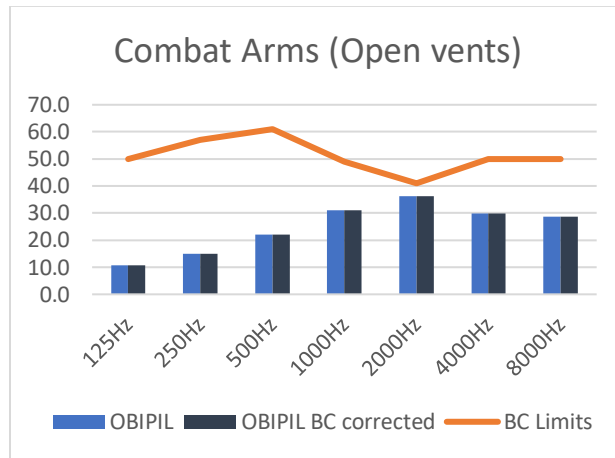


Figure 25: OBIPIL versus BC limits for the 3M Combat Arms earplugs with open vents

In this case, the comparison between the measured versus the estimated HPD parameters, presented in Table 8, is not showing a big difference. The small variation between both scenarios is induced by eq.28 which calculates the SPL at the eardrum only with sub-bands between 125 Hz and 8 kHz.

Table 8 : Measured versus estimated HPD performances

Combat Arms (Open vents)	IPIL	$AN E_{effect}$
Measured HPD performance	32.7(1.8) dB	5825
BC Corrected HPD performance	32.7 dB	5860

Some results illustrating the measurements results and the calculations are presented in Annex C.

### 4.3.2. Results when the HPD is the Combat Arms Earplugs Gen IV with CLOSED vents

Results in Fig.26 show that the tested HPD was BC corrected at 2 kHz, and in fact the OBIPIL amplitudes did not exceed the BC limits for a non-covered head for most of the OBs, except at 2 kHz.

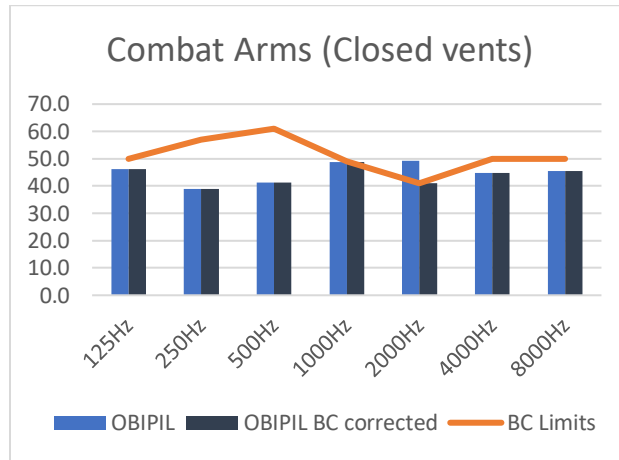


Figure 26: OBIPIL versus BC limits for the 3M Combat Arms earplugs with closed vents

In this case, and as shown by Table 9, the estimated IPIL was capped at about 42dB and the ANE value was reduced to about 50.000 shots.

Table 9: Measured versus estimated HPD performances

Combat Arms (Closed vents)	IPIL	ANE
HPD performance ATF measured	47.8(3.2) dB	187828
HPD performance BC corrected	41.9 dB	49183

Some results illustrating the measurements results and the calculations are presented in Annex C.

### 4.3.3. Results when the HPD is the Superfit 30 Earplug

Results in Fig.27 show that the tested HPD was BC corrected at 2 kHz. Again the OBIPIL amplitudes did not exceed the BC limits for a non-covered head for most of the OBs, except at 2 kHz.

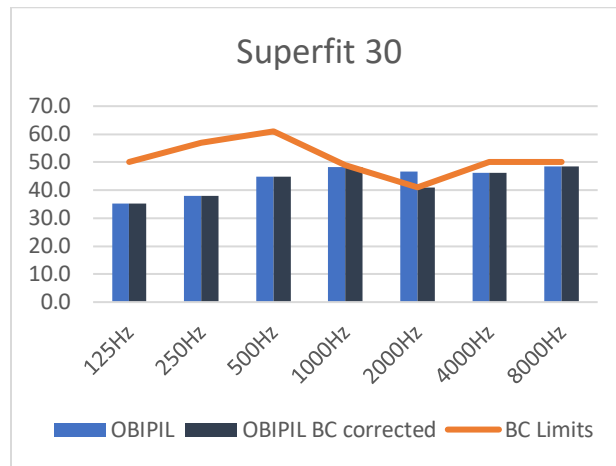


Figure 27: OBIPIL versus BC limits for the Superfit 30 earplug

In this case, and as shown by Table 10, the estimated IPIL was capped at about 42dB and the ANE value was reduced to about 50.000 shots.

Table 10: Measured versus estimated HPD performances

Superfit 30	IPIL	ANE
HPD performance ATF measured	46.9(2.1) dB	153017
HPD performance BC corrected	42.1 dB	50753

Some results illustrating the measurements results and the calculations are presented in Annex C.

#### 4.3.4. Results when the HPD is the X5A ear muff

Results in Fig.28 show that the tested HPD doesn't need to be BC corrected. In fact, the OBIPIL amplitudes did not exceed the BC limits for a non-covered head.

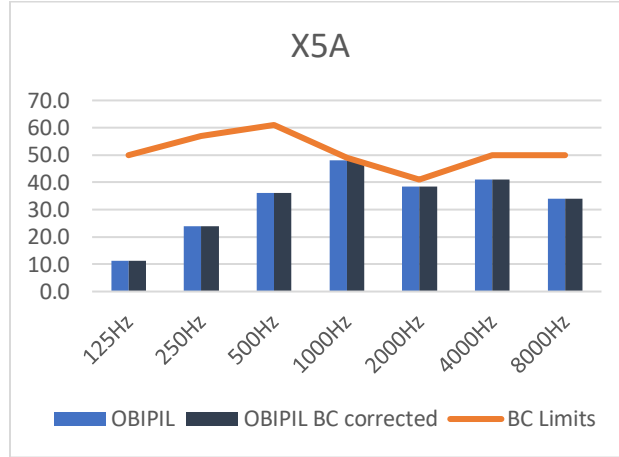


Figure 28: OBIPIL versus BC limits for the Superfit 33 earplug

In this case, the comparison between the measured versus the estimated HPD parameters, presented in Table 11, is not showing a big difference. The small variation between both scenarios is induced by eq.28 which calculates the SPL at the eardrum only with sub-bands between 125 Hz and 8 kHz.

Table 11: Measured versus estimated HPD performances

<b>X5A</b>	<b>IPIL</b>	<b>ANE</b>
HPD performance ATF measured	37.8(2.3) dB	19125
HPD performance BC corrected	38.4 dB	21813

Some results illustrating the measurements results and the calculations are presented in Annex C.

**4.3.5. Results when the HPD is the X5A ear muff combined with the Combat Arm earplugs with open vents**

Results in Fig.29 show that the tested HPD was BC corrected for the OBs higher than 1 kHz.

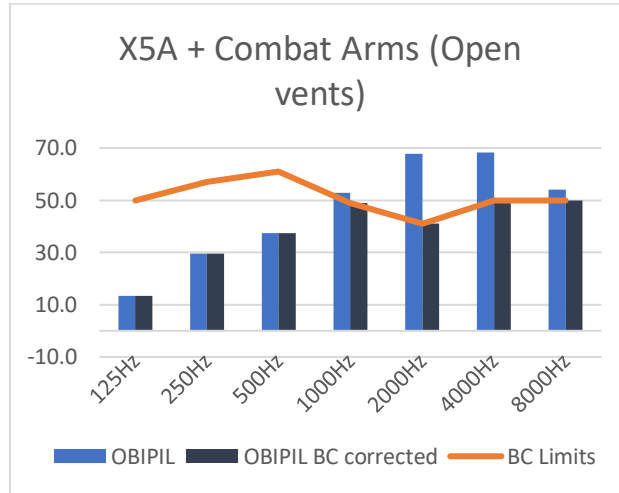


*Figure 29: OBIPIL versus BC limits for the Combat Arms earplugs with open vents & X5A earmuffs when used together for double protection*

In this case, and as shown by Table 12, the estimated IPIL was capped at about 42dB and the ANE value was reduced to about 50.000 shots.

*Table 12: Measured versus estimated HPD performances*

<b>X5A + Combat Arms (Open vents)</b>	<b>IPIL</b>	<b>ANE</b>
HPD performance ATF measured	44.1(1.9) dB	80716
HPD performance BC corrected	41.6 dB	45330

Some results illustrating the measurements results and the calculations are presented in Annex C.

**4.3.6. Results when the HPD is the X5A ear muff combined with the Combat Arm earplugs with closed vents**

Results in Fig.30 show that the tested HPD was BC corrected for the OBs higher than 1 kHz.

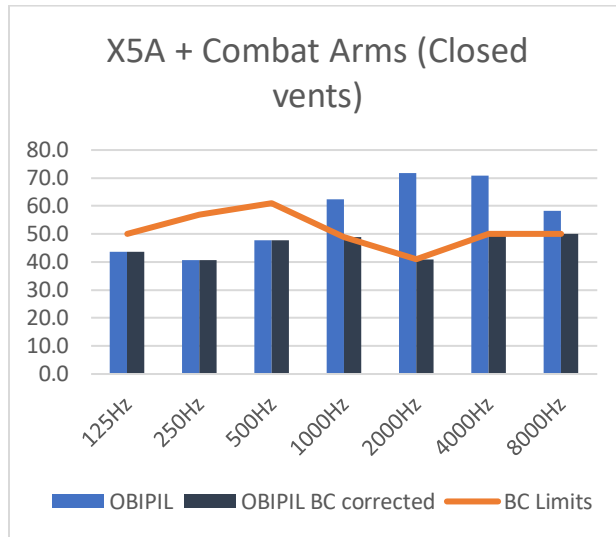


*Figure 30: OBIPIL versus BC limits for the Combat Arms earplugs with closed vents & X5A earmuffs when used together for double protection*

In this case, and as shown by Table 13, the estimated IPIL was capped at about 42dB and the ANE value was reduced to about 50.000 shots.

*Table 13: Measured versus estimated HPD performances*

<b>X5a + Combat Arms (Closed vents)</b>	<b>IPIL</b>	<b>ANE</b>
HPD performance ATF measured	52.2(2.1) dB	526990
HPD performance BC corrected	42.4 dB	54660

Some results illustrating the measurements results and the calculations are presented in Annex C.

#### 4.3.7. Results when the HPD is the X5A ear muff combined with the Superfit 30 earplugs

Results in Fig.31 show that the tested HPD was BC corrected for the OBs higher than 1 kHz.

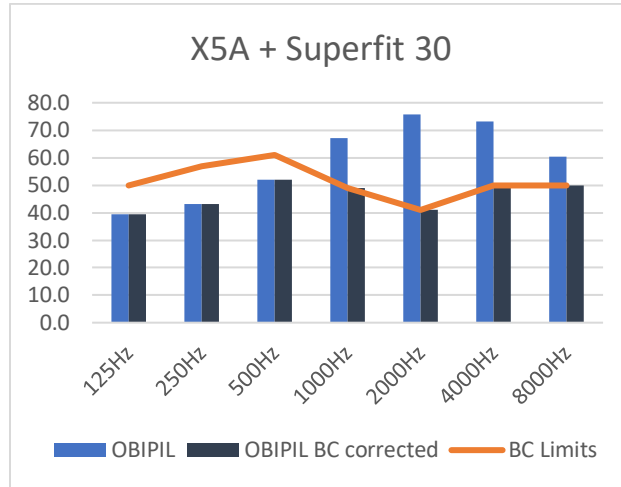


Figure 31: OBIPIL versus BC limits for the Superfit 30 earplugs with closed vents & X5A earmuffs when used together for double protection

In this case, and as shown by Table 14, the estimated IPIL was capped at about 42dB and the ANE value was reduced to about 50.000 shots.

Table 14: Measured versus estimated HPD performances

<b>X5A + Superfit 30</b>	<b>IPIL</b>	<b>ANE</b>
HPD performance ATF measured	58.1(1.9) dB	2037080
HPD performance BC corrected	42.4 dB	54772

Some results illustrating the measurements results and the calculations are presented in Annex C.

## 4.4. Discussion

(A)

The proposed OBIPIL tool is very helpful to predict the behavior of the HPDs at different OBs and when the HPD is exposed to a high-level impulse noise. This new metric led us to propose a BC correction approach adjusting the IPIL measured with an ATF to the limitations imposed by the human auditory system. However, the proposed BC correction approach remains simplistic and may not be sufficient because:

- The BC limits were established using steady-state noise test conditions [5];
- More modelling effort is needed to understand how the human BC conduction pathways are behaving to transfer the sound to the cochlea [8], and then a better correction approach should be proposed in order to get a more realistic estimation for the IPIL and the ANE;
- There is a phase shift between the signal transferred to the cochlea via the HPD and the signal transferred to the cochlea via the skull [8].

(B)

The results are showing that the BC correction approach induced a capping for the IPIL at about 42 dB. Fig.32 compares between IPIL values measured with the ATF against IPIL values when BC is corrected.

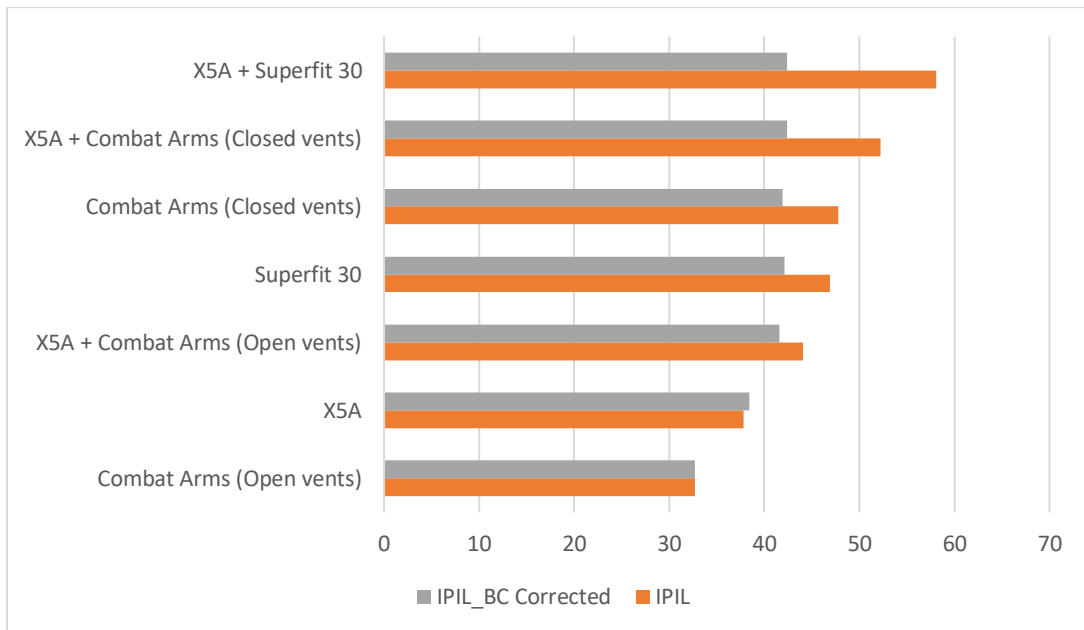
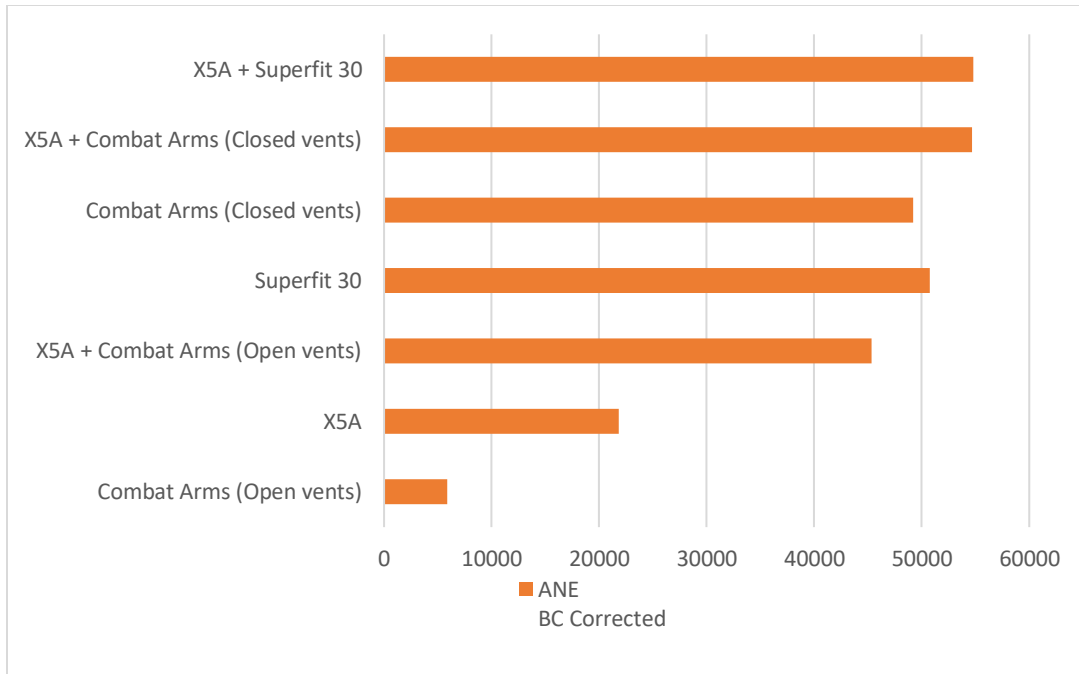


Figure 32 : IPIL versus IPIL BC Corrected for the tested HPDs

Since the ANE estimation depends on the value of the IPIL, and because the IPIL is capping at 42 dB, then ANE is saturating at about 50000 shots as expressed by Fig.33.



*Figure 33 : ANE when BC corrected for the tested HPDs*

These results do not contradict the literature [28], which proposes the 41 dB at 2 kHz as a limit to apply to the measured IPIL when the ATF is uncovered. In fact, in this research work the ATF was uncovered. However, the question that was not answered yet in this study is:

How robust would this evaluation approach be when dealing with impulse noise generated by many other small firearms, other artillery pieces or by using an acoustic shock tube?

## 4.5. Conclusion

A method based on attenuation in octave bands (OBIPIL) is proposed to assess HPD protection level with impulse noises. In addition, the comparison of the OBIPIL results with the BC limits allows an estimation of the effectiveness of the protection level at each OB. Therefore, it becomes possible to compare the effectiveness of different HPD combinations and to propose better test and design future systems. Measurements of the IPIL and the OBIPIL for several types of HPD systems were performed during weapons firing. Although the measurements were performed using a modified version of the ANSI/ASA S12.42 standard, the results did provide a comparison of different types of HPDs in the time-frequency domain for an operationally relevant noise source, i.e. small arms. While the IPIL captures information from only two peak values, the OBIPIL allows analysis of HPD attenuation over the OB spectrum, and leads to a BC correction approach estimating an IPIL and ANE values constrained by the physiological travel of sound using multiple bone pathways.

As a result, the OBIPIL allows for potential improvements in modeling the impulse noise impact on hearing.

## Chapter 5 - GENERAL DISCUSSION

In this section, a summary of the limitations and future work identified throughout this thesis is provided in the following table.

*Table 15 : Limitations and future work*

<b>Limitation</b>	<b>Future work</b>
<p>(eq.11) The Equal Energy Model [18; 50] tried to correlate between some standard noise measurements and hearing loss [51]. It is built on the assumption that the risk of hearing loss produced by impulse noises will be monotonically increasing as the total A-weighted energy received by an experimental subject increases [52]. However, most of the international standards would recommend limiting the 8-hour exposure to less than 85 dBA.</p>	<p>The equal energy model has been used as the main approach for this thesis, and the introduction of the OBIPIL calculation method opened the door to introduce the BC correction concept, adjusting the IPIL value to the human physiological limitations. Comparing the obtained results with the AHAH model [17], and possibly with other models, will be necessary to study the limitations and the possible improvements for the work presented herein.</p>
<p>The attenuation properties of the HPDs are normally measured by the manufacturer according to existing standards using fixed-frequency steady state noises. The manufacturer doesn't provide any information about the attenuation performance of these HPDs under high level impulse noises, and hence, the level of protection offered under high level impulse noise is unknown [2; 39].</p>	<p>For continuous improvements, the outcome of this OT&amp;E study impacts the DT&amp;E by defining new specific performance requirements and goals. In fact, while the IPIL captures information from only two peak values, the OBIPIL allows analysis of HPD attenuation over the OB spectrum. As a result:</p> <ul style="list-style-type: none"> <li>- More potential is now available to improve the modelling and design of new HPD systems.</li> <li>- Developing a new performance criterion based on OBIPIL, for new HPD systems, is now possible.</li> </ul>
<p>(eq.17) The TFOE is assumed not changing between measurements for a given noise source and measurement configuration. In addition, the TFOE calculation method is assuming that the system is linear.</p>	<p>A better calculation approach of the TFOE is needed to confirm the linearity of the system when the PPL varies by +/- 3 dB. In fact, the linearity of the system is not guaranteed when impulse noise levels are higher than 140 dBP.</p>

<b>Limitation</b>	<b>Future work</b>
This study assumes that level dependent HPDs are providing the same attenuation level at 1m from the MO as when the measurement test is performed at the MO location.	Studying the linearity of the HPDs under high level impulse noise is necessary to predict the attenuation behavior of the HPDs at the MO location.
The sequential T&E strategy is now a candidate for IL measurements when dealing with reverberant test environments. But it has not been validated in such environments yet.	Further tests are needed to confirm this assertion.
(eq.20) Considering the need to compensate for the measurements standard deviation and accounting for possible minimal losses because of fitting issues encountered by trained personnel, a realistic protection should be 3 dB below the measured IPIL [21; 22], which means that a realistic ANE must be cut by 50% .	Practically measuring the IPIL value depends on the fit between the HPD and the hearing system during the test experiment. The fit during the test experiment is assumed to be high, but less high for trained people and low for non-trained people. An investigation is needed to estimate the acceptable dB drop, based on the user physiology and on the experimental test conditions.
(eq.27) The BC correction approach assumes that as soon as the BC attenuation limits are exceeded by the HPD attenuation capabilities, then the extra HPD attenuation capability exceeding the BC limits does not provide an additional protection to the cochlea.	So far, current reports about using BC have focused only on taking advantage from these sound pathways to propose new innovative communication methods [59] for steady state noise types. Moreover, the BC limits used in this study were measured under steady state noise conditions [5] and not under impulse noise conditions. The new concept of the BC corrected approach, presented in this thesis, needs more work to confirm that the proposed BC correction approach estimating the corrected IPIL and ANE, is acceptable or accurate.
(Eq.28) The reconstruction of the IPIL has been limited to the usage of the sub-signals ranging between 125 Hz to 8000 Hz, to match the same frequency range of the BC limits reported in the literature [5].	More work is needed to assess the impact of this limitation on the acceptability and the accuracy of the BC correction approach.

<b>Limitation</b>	<b>Future work</b>
-------------------	--------------------

<p>There is a phase shift between the signal transferred to the cochlea via the HPD and the signal transferred to the cochlea via the skull [8].</p>	<p>The spectral BC measurements [5] don't include any information about how this spectral characterization impacts the phase of an excitation signal; therefore, more work is needed to review and improve the test plan used to generate the BC attenuation limits.</p>
<p>The BC correction method proposed in this thesis is assumed to be robust enough to estimate a corrected IPIL limit when dealing with different weapon systems (e.g. small firearms fitted with suppressors) radiating an acoustic wave with different energy distribution over the spectrum. (see * below)</p>	<p>Future work is needed to confirm the robustness of the proposed BC correction method over a large selection of small firearms configuration systems..</p>

(\*) When applying the Matlab scalogram function on the signal measured at the MO location and when the same small firearm is fitted with and without a suppressor; the results shows that:

- The spectral magnitude distribution of the acoustic waveform is high at 2 kHz when the small firearm is not fitted with a suppressor, as shown in Fig.34.
- The main spectral magnitude distribution at 2 kHz has been shifted to frequencies higher than 4 kHz when the small firearm is fitted with a suppressor, as shown in Fig.34.

**Without Suppressor**

**With Suppressor**

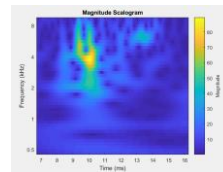
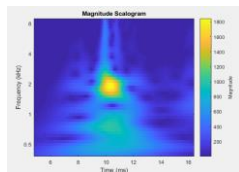


*Figure 34: Acoustic spectral magnitude distribution at the MO location when the SA is fitted with and without a suppressor*

The scalogram shows that when the small firearm is not fitted with a suppressor the energy of the signal is centered around 2 kHz; however, at 2 kHz the BC limit is 41 dB. Consequently, using 41 dB as a BC limit in the literature [28] is justified for small firearms.

The problem now is that when using a suppressor, the energy content of the radiated acoustic signal shifts to higher frequencies, and the magnitude of the signal drops drastically compared to the case when the suppressor is not used.

The questions that should be answered are thus:

- Is using the 41dB as a BC limit always valid when the signal energy shifts to higher frequencies?
- Is the OBIPIL based evaluation approach good enough to estimate the new BC limit?
- Is the OBIPIL based evaluation approach good enough to estimate new DRC for this new operational condition?

## Chapter 6 - GENERAL CONCLUSION

Given the increasing need for evaluating new HPD systems (e.g., vented earplugs, electronic noise reduction devices) and configurations (e.g., helmet with earplugs, ear muff with earplugs) under impulse noise conditions, the OBIPIL method was introduced in this thesis.

In addition, the comparison of the OBIPIL results with the BC limits allows an estimation of the effectiveness of the protection level at each OB. Therefore, it becomes possible to compare the effectiveness of different HPD combinations and to propose a method to BC-correct the IPIL measurements, performed initially with an ATF, to meet the human physiological limitations.

In fact, in this thesis, new T&E techniques have been proposed to characterize HPDs when exposed to an impulse noise from a specific small firearm, opening the opportunity for defining new performance requirements.

The testing approach, presented in chapter 3, is proposing a new test validation alternative based on ANSI/ASA S12.42-2010, for testing HPDs when the impulse noise is generated by a small firearm. This new testing approach:

- Increases the measurement reliability when dealing with a non-spherical acoustic radiation;
- Offers a robust approach for measuring the IPIL, when the radiated noise wave is non-spherical, and the proposed approach could be very useful when measuring noise in reverberant test environments;
- Assesses the HPDs in an operational-like testing setup.

The evaluation approach, presented in chapter 4, introduces a new evaluation strategy using a sub-band analysis for dealing with impulse noise generated by a small firearm. This new evaluation approach:

- Introduces the new concept of OBIPIL, a calculation tool gauging HPD protection capabilities in the OB domain; this method gives more granularity than the IPIL, and in fact it estimates the HPDs protection capability at each OB;
- Introduces a new and innovative BC correction approach, OBIPIL-based, to correct the IPIL value by considering the physiological human limits, hence a more realistic ANE is then computed and proposed.

Pros, cons and avenues for future work related to each of the above-mentioned points were also analyzed and discussed in this thesis.

## REFERENCES

- [1] Sharon M. Abel; “Risk factors for the development of noise- induced hearing loss in Canadian Forces personnel”; DRDC, Toronto, September 2004, ECR 2004-116
- [2] Ann Nakashima, Sadri Sarray, Nir Fink; “Insertion loss of hearing protection devices for military impulse noise”; Canadian Acoustical Association, 2017, Vol 45 No 3
- [3] American National Standards Institute, Acoustical Society of America. ANSI/ASA S12.42-2010, “Methods for the measurement of insertion loss of hearing protection devices in continuous or impulsive noise using microphone-in-real-ear or acoustic test fixture procedures”. Melville (NY); 2010.
- [4] Bruce E.Amrein, Tomasz R.Letowski; “Predicting and ameliorating the effect of very intense sounds on the ear : The Auditory Hazard Assessment Algorithm for Humans (AHAH)”; NATO, Jan 2011, RTO-MP-HFM-207
- [5] Elliott H. Berger, Ronald W.Kieper; “Hearing protection: Surpassing the limits to attenuation imposed by the bone conduction pathways”; J. Acoust. Soc. Am., October 2003, Vol. 114, No. 4, Pt. 1,
- [6] Elliott H. Berger; “Preferred Methods for Measuring Hearing Protector Attenuation”; Environmental Noise Control, The 2005 Congress and Exposition on Noise Control Engineering, Rio de Janeiro (Brazil) , 07-10 August 2005
- [7] Nir Fink, Hagar Zvia Pikkell, Arik Eisenkraft, and Gregory A. Banta; “Hearing protection devices and methods used for their evaluation: A military perspective”; Journal of Military, Veteran and Family Health, 5(1) 2019 doi:10.3138/jmvfh.2017-0034
- [8] Anthony J. Dietz, Ph.D., B. Scott May, Ph.D., Darin A. Knaus, Ph.D., Harold P. Greeley; “Hearing Protection for Bone-Conducted Sound”; NATO, Neuilly-Sur-Seine (France), Apr 2005, RTO-MP-HFM-123, paper 14, (pp. 14-1 – 14-18)
- [9] Aage R. Moller, “Hearing. Its Physiology and Pathophysiology”. Academic Press, 1 edition, ISBN-13: 978-0125042550 , 08 June 2000
- [10] Brent Edwards; “Speech Processing in the Auditory System - Hearing Aids and Hearing Impairment”; Springer ISBN 978-1-4419-1831-4
- [11] Graeme Clark; “Speech Processing in the Auditory System - Cochlear Implants”; Springer ISBN 978-1-4419-1831-4
- [12] Juan D. Goutman, A. Belen Elgoyhen, Maria E. Gómez-Casati; “Cochlear hair cells: the sound-sensing machines”; Elsevier. 31 Aug 2015. FEBS Letters 589 (2015) 3354–3361
- [13] “Systems Engineering Handbook”, INCOSE-TP-2003-002-03.2.2 , Oct 2011
- [14] “Test and Evaluation management guide”, January 2005, Fifth Edition, The Defense Acquisition University Press, Fort Belvoir (USA) VA 22060-55654.
- [15] Sadreddine Sarray, Ann Nakashima, Hilmi R.Dajani, Martin Bouchard, David Lo, Sebastian Ghinet; “Octave Band Peak Insertion Loss: A Method To Characterize Hearing Protection Devices When Firing With Small Arms”; ICSV26, 7-11 July 2019

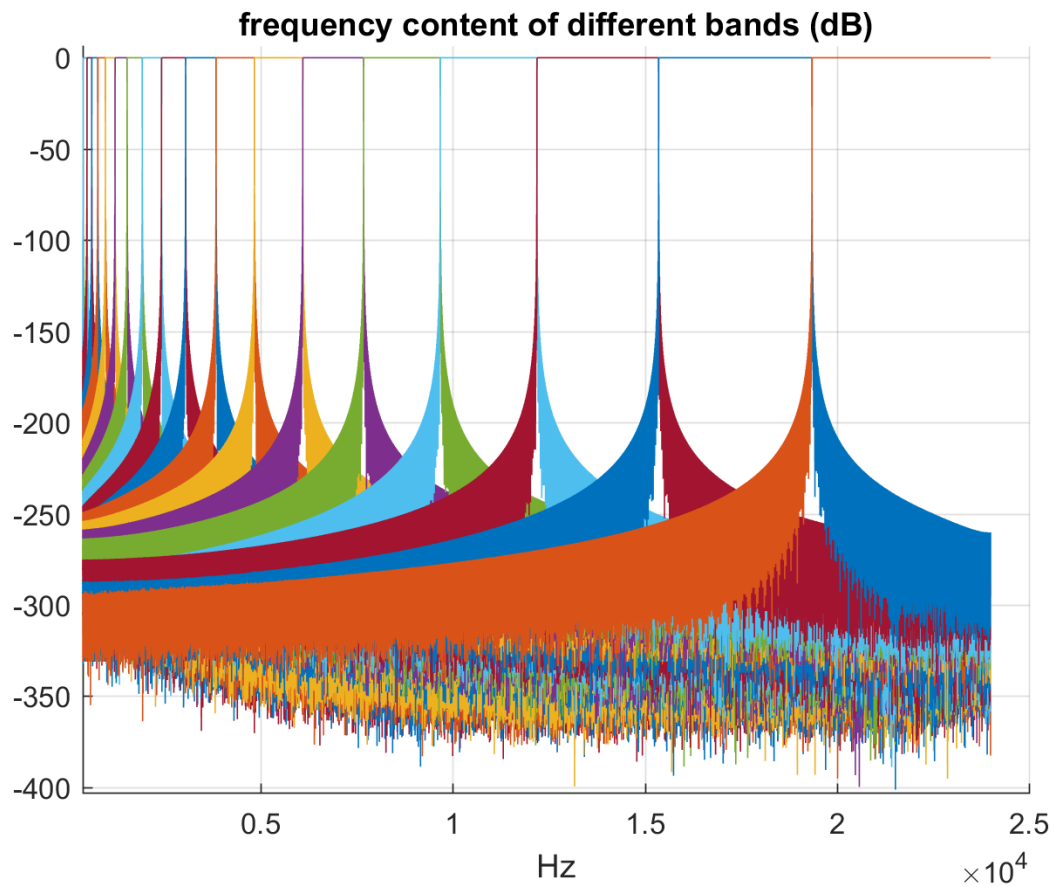
- [16] National Defence; “GENERAL SAFETY PROGRAM – VOLUME 2 – GENERAL SAFETY STANDARDS – Chapter 10”; MDN Canada ; 2003-01-01; C-02-040-009/AG-001
- [17] MIL-STD-1474E. (2015); “Department of Defense, Design Criteria Standard, Noise Limits”; Washington DC (USA), 2015.
- [18] Christian Giguere, Chantal Laroche; “Hearing Loss Prevention Program In The Military Environment”; Canadian Acoustics; 2005 ; 21-Vol.33 No.4
- [19] Lewis H. Bell, Douglas H. Bell; “Industrial Noise Control - Fundamentals and Applications”; CRC Press LLC Second Edition , October 1993, ISBN 0-8247-9028-6
- [20] Gerald Baillargeon; “Techniques Statistiques”; Les Editions SMG; 1984 ; ISBN 2-89094-027-6
- [21] Kuba Mazur, Jeremie Voix; “Development of an Individual Dosimetric Hearing Protection Device”; Inter.Noise 2012, 19-22 Aug 2012
- [22] Richard Neitzel , Noah Seixas ;“The effectiveness of hearing protection among construction workers” Journal of occupational and environmental hygiene; 2005 ; Vol.2(4); pp. 227-38.
- [23] Julie A. Norin, Diana C. Emanuel, Tomasz R. Letowski; “Speech Intelligibility and Passive, Level-Dependent Earplugs”; Ear and Hearing ; March 2011; Vol.32, No.5, pp. 642-649.
- [24] CSA Standard Z94.2-14 ; “Hearing protection devices Performance, Selection, Care, and Use”; Canadian Standards Association ; Toronto ; 2014.
- [25] Chief of Staff – Medical Services; “Hearing Conservation Program”; Washington DC (USA); 10 Dec 1998; DA PAM 40–501
- [26] National Defense; “OPERATIONAL TRAINING - Training Safety”; MDN Canada; 2004; B-GL-381-001/TS-000
- [27] Minister of Justice; “Canada Occupational Health and Safety Regulations”; Canada; 4 Aug 2015; SOR/86-304
- [28] Amir Khan, Cameron J. Fackler, William J. Murphy; “Comparison of Two Acoustic Test Fixtures for Measurement of Impulse Peak Insertion Loss”; NIOSH; USA; Nov 2013; EPHB Report No. 350-13a
- [29] Bureau Of Medicine and Surgery; “Summary of HPD use requirements”; Department of the Navy (USA); 13 Dec 2012 ; BUMED NOTICE 6260
- [30] U.S. Dept. of Health and Human Services; “The NIOSH compendium of hearing protection devices”; DHHS publication; Atlanta (GA); 1994; Series (NIOSH) 95-105
- [31] International Organization for Standardization ; “Acoustics – hearing protectors – Part 2: Estimation of Effective A-weighted sound pressure levels when hearing protectors are worn”; (10-2018); ISO 4869-2:2018.
- [32] Cameron J. Fackler, Elliott H. Berger, William J. Murphy, and Michael E. Stergar; “Spectral analysis of hearing protector impulsive insertion loss”; International Journal of Audiology; (2016); 56(SUP1): 1–9.
- [33] Julius O.Smith; “Audio FFT Banks”; Conference on Digital Audio Effects (DAFx-09), Como, Italy, September 1-4, 2009.
- [34] Oi Saeng Hong, Madeleine J. Kerr, Gayla L. Poling, Sumitrajit Dhar; “Understanding and preventing noise-induced hearing loss”; Elsevier 2013.

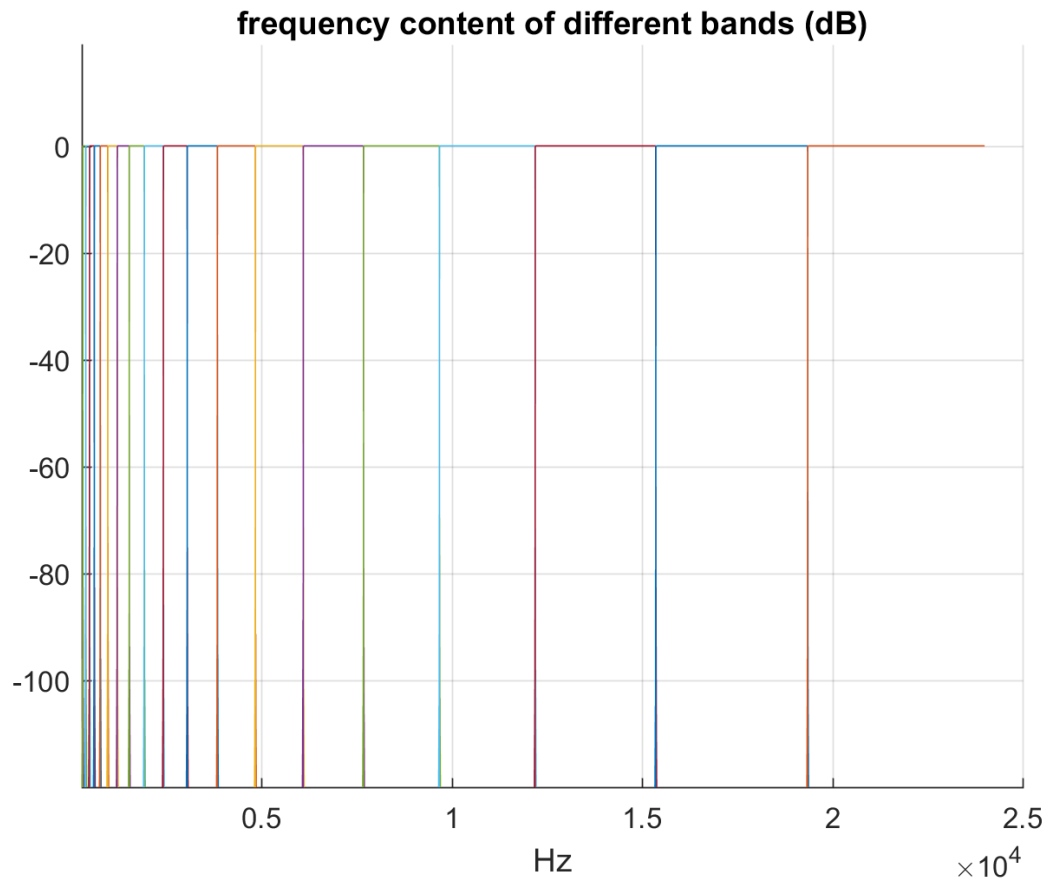
- [35] Noam Yehudai, Nir Fink, Manor Shpriz, Tal Marom; “Acute Acoustic Trauma among Soldiers during an Intense Combat”; Journal of the American Academy of Audiology;2016
- [36] Ann Nakashima; “A comparison of metrics for impulse noise exposure”. DRDC; Toronto; 2015; DRDC-RDDC-2015-R243.
- [37] Peter Teague, James Conomos and Vasos Alexandrou; “Overview of Developments in the Description and Assessment of High Intensity Impulse Noise Exposure”; Proceedings of Acoustics 2016, Brisbane (Australia); 9-11 Nov 2016.
- [38] Ann Nakashima, Rocco Farinaccio; “Review of Weapon Noise Measurement and Damage Risk Criteria: Considerations for Auditory Protection and Performance”; Military Medicine 2015.
- [39] Ann Nakashima; “Impulse Noise: Measurement Techniques and Hearing Protector Performance”, DRDC 2006.
- [40] Roger P. Hamernik; William A. Ahroon; Keng D. Hsueh; “The energy spectrum of an impulse: its relation to hearing loss”; Acoustical Society of America; 1991.
- [41] Hongyuan Jiang. “Nonlinear Sound Absorption Performance of Metal Rubber Material”. Journal of Mechanical Engineering, October 2010.
- [42] Annalisa De Paolis, Marom Bikson, Jeremy T.Nelson, J.Alexander de Ru, Mark Packer, Luis Cardoso; « Analytical and numerical modeling of hearing system : Advances towards the assessment of hearing damage »; Elsevier 2017
- [43] Aage R. Moller, “Intra-Aural Muscle Contraction in Man, Examined by Measuring Acoustic Impedance of the Ear”. Laryngoscope, LXVIII; 1958; 48-62
- [44] Aage R. Moller, “The Acoustic Reflex in Man”. J. Acoust. Soc. Am.; 1962; (34): 1524-1534.
- [45] Aage R. Moller, “The Acoustic Middle Ear Muscle Reflex”. Handbook of Sensory Physiology, edited by W.D. Keidel and W.D. Neff. New York: Springer-Verlag, 1974, pp. 519-545.
- [46] Aage R. Moller, “Hearing. Its Physiology and Pathophysiology”; Academic Press, San Diego; 2000
- [47] Sunil Puria, Charles R. Steele; “HANDBOOK OF THE SENSES : Chapter 7: Mechano-Acoustical Transformations”; Semantic Scholar ; 2007
- [48] American National Standards Institute. ANSI S1.11-2004: Specification for octave-band and fractional-octave-band analog and digital filters. Melville (NY); 2004;
- [49] Won Joon Song; “Study on Human Auditory System Models and Risk Assessment of Noise Induced Hearing Loss”; University of Cincinnati; 2010.
- [50] ISO 1999:2013; “Acoustics - Estimation of noise-induced hearing loss”;
- [51] G. Richard Price, Joel T. Kalb; « The Philosophy, Theoretical Bases, and Implementation of the AHAHAH Model for Evaluation of Hazard from Exposure to Intense Sounds »; ARL 2018;
- [52] Qinq Wu; “Characterization of Impulse Noise and Hazard Analysis of Impulse Noise Induced Hearing Loss using AHAHAH Modeling”; Southern Illinois University Carbondale ; 2014
- [53] [https://en.wikipedia.org/wiki/Acoustic\\_resonance](https://en.wikipedia.org/wiki/Acoustic_resonance) ; (2019)
- [54] Yoiti Suzuki, Hiashi Takeshima ; “Equal-loudness-level contours for pure tones”; J. Acoust. Soc. Am., 2004.
- [55] Bruel and Kjaer; “Measuring Sound”; BR0047-13

- [56] Michael Möser ; “Engineering Acoustics: An Introduction to Noise Control”; Springer Second Edition ; 2009 ; Chapter 1..
- [57] [“https://en.wikipedia.org/wiki/Octave”](https://en.wikipedia.org/wiki/Octave); (1999)
- [58] D. Strelhoff, A. Flock, K.E. Minser; "Role of inner and outer hair cells in mechanical frequency selectivity of the cochlea"; Elsevier - Hearing Research; May 1985; Volume 18, Issue 2, Pages 169-175
- [59] Maranda McBride, Phuong Tran, and Tomasz Letowski; “Bone Conduction Communication : Research Progress and Directions”; US Army Research Laboratory, Aug 2017; ARL-TR-8096
- [60] Hamed Samimi; “Automatic Recognition of Speech-Evoked Brainstem Responses to English Vowels”; University of Ottawa ; 2015
- [61] Chanwoo Kim; “Signal processing for robust speech recognition - motivated by auditory processing”; Carnegie Mellon University; 2010
- [62] National Defence; “Operational Training : Training Safety”; Canada, 2004, MOD 9-2007-01-26 , pp.104-121

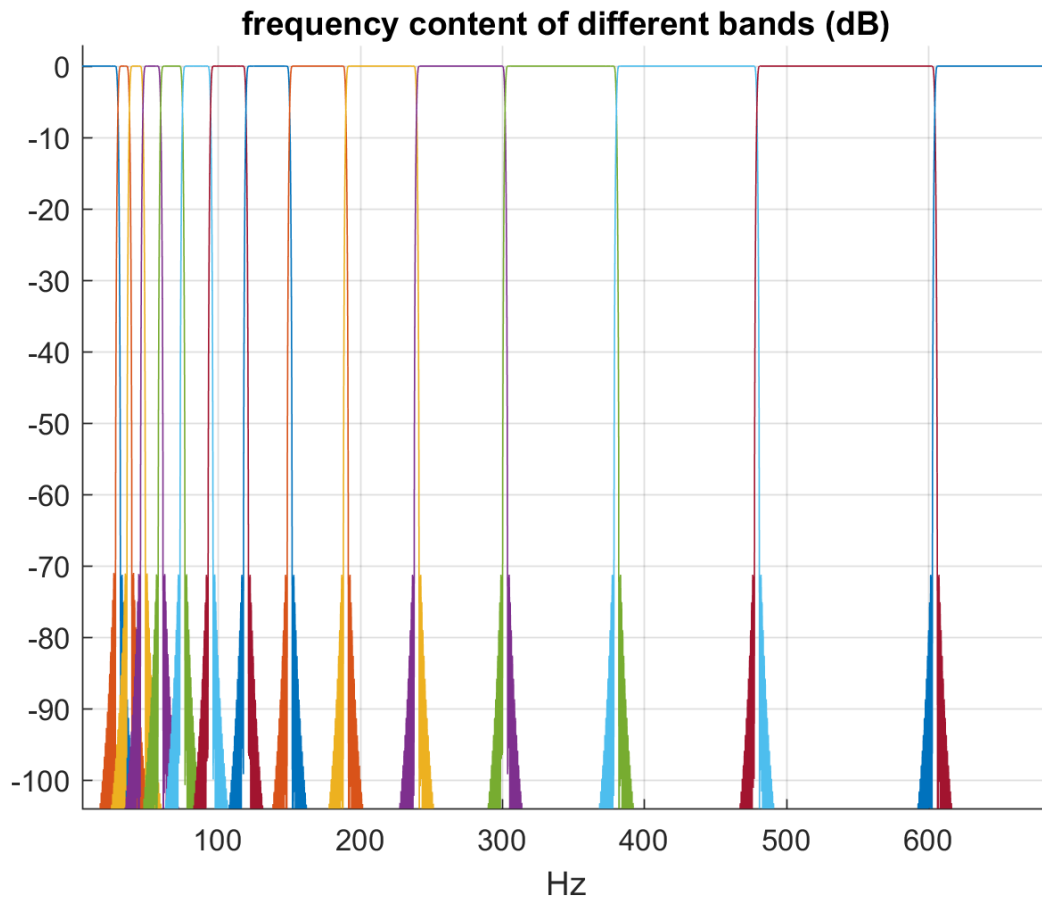
## ANNEX A – Time and frequency domain performances of the OB Filter Bank

Illustration of the magnitude response of the different sub-bands (3 first plots below), for a signal with Nyquist frequency 24 kHz. We see that the  $1/3^{\text{rd}}$  octave decomposition is near perfect: very little interference between bands, and flat response within a band.



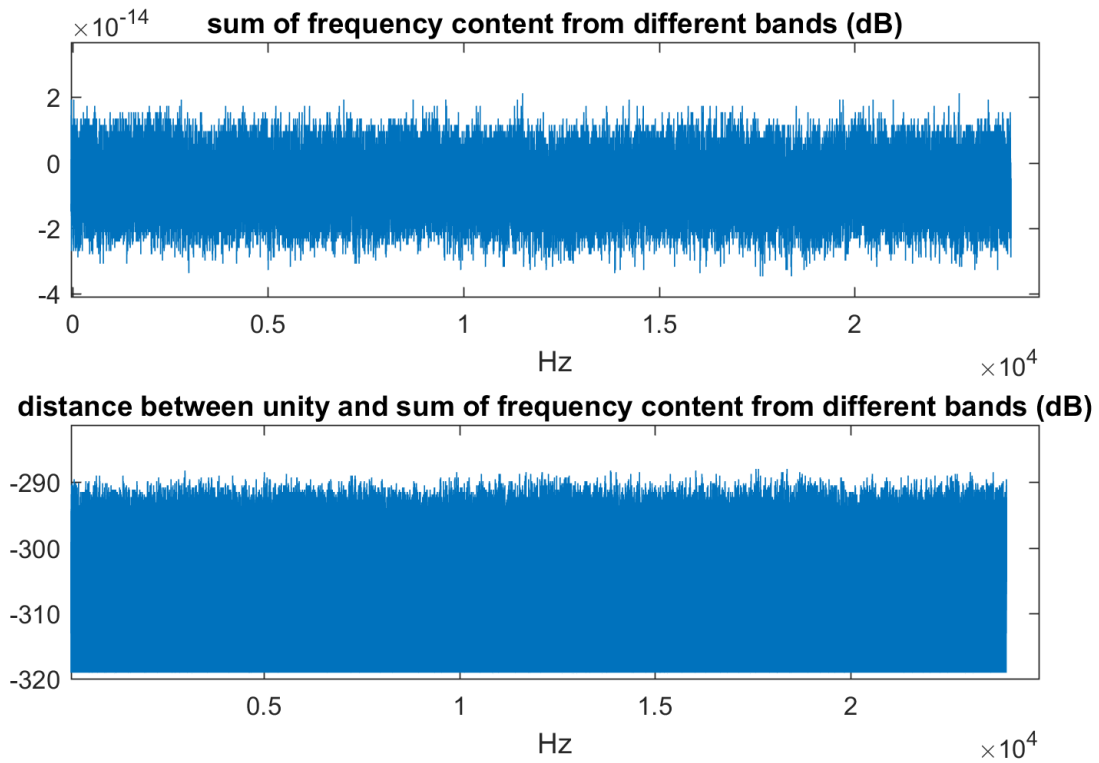


Zooming at lower frequency bands:

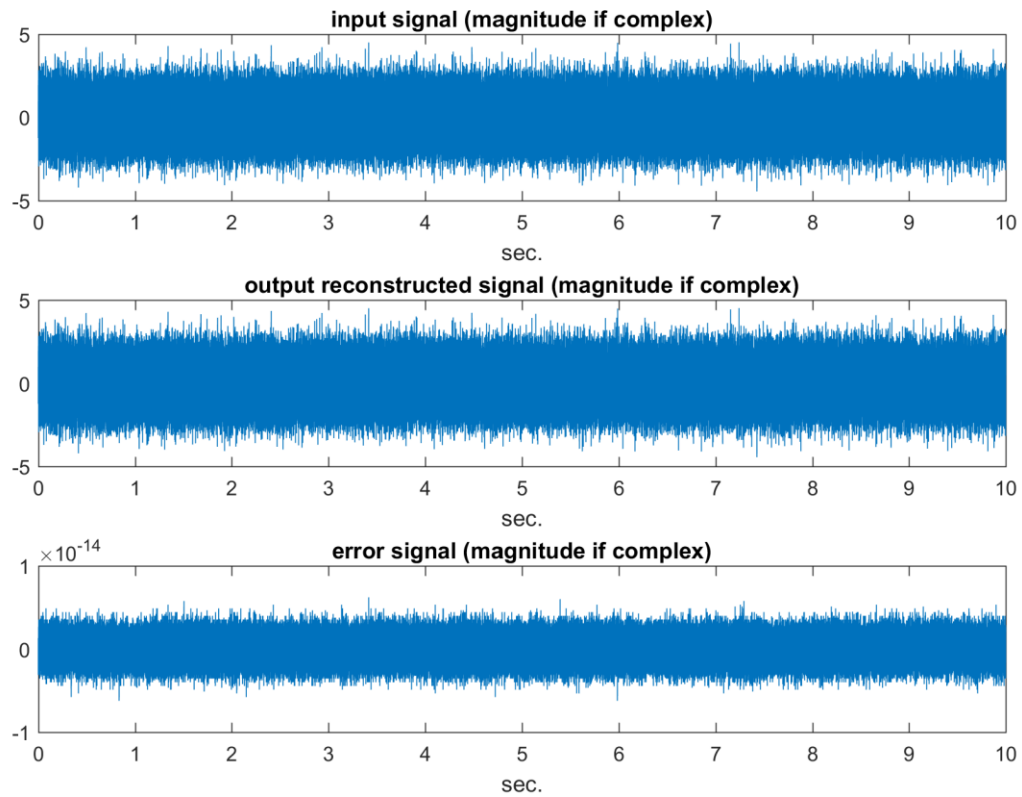


The first plot below shows the magnitude of the sum of all the frequency responses from the sub-bands, for a Nyquist frequency 24 kHz. We see that the result in dB is nearly unity (0 dB, only  $10^{-14}$  dB error).

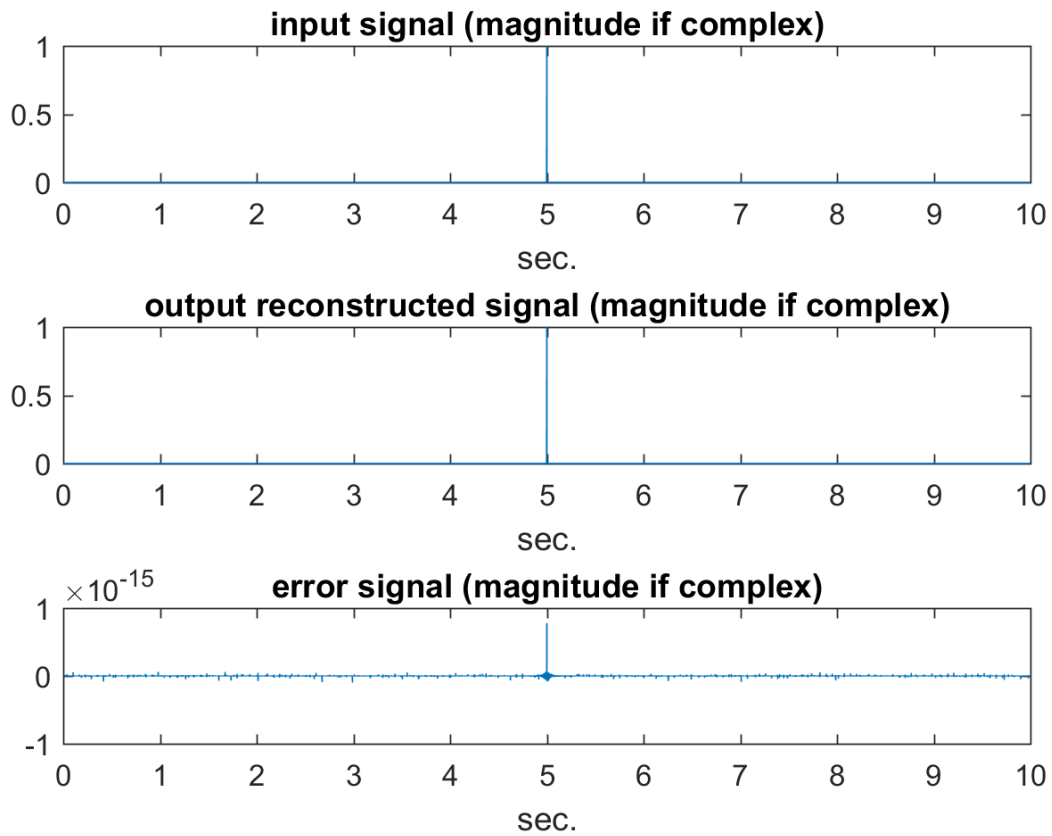
The second plot shows the magnitude response when a perfect unit response is subtracted from the sum whose magnitude is plotted in the first plot. The very small result (-300 dB) is another indication of the near perfect response of the filter bank.



Comparison of input signal and output signal (sum of all sub-band output signals) for the case where the input is 10 seconds of Gaussian white noise. We see that the error (difference) between the two signals very small (order  $10^{-14}$ ), illustrating the perfect reconstruction property of the filter bank.



Comparison of input signal and output signal (sum of all sub-band output signals) for the case where the input is a unit sample located at 5 sec. We see again that the error (difference) between the two signals very small (order  $10^{-15}$ ), illustrating the perfect reconstruction property of the filter bank.



## ANNEX B – Statistical methods and data presentation

- The data format used in this thesis follows the following format:

Average of the Magnitude in dB (Standard Deviation in dB)

- The reported measurements per trial, e.g. IPIL, PPL, are independent variables. Herein X represents the set of measurements at the left ear, Y represents the set of measurements at the right ear, and Z represents the set of IPIL measurements for both ears.

By assuming that the measurements are normally distributed and by considering that the fit between the HPD system at each ear is never identical [20], this leads to the following calculation of the mean, the variance  $\sigma^2$ , and the standard deviation,  $\sigma$ , values per trial.

Left ear calculation

$$X = \{x_1, x_2, x_3, x_4, x_5\}$$

$$\mu_x, \sigma_x^2$$

Right ear calculations

$$Y = \{y_1, y_2, y_3, y_4, y_5\}$$

$$\mu_y, \sigma_y^2$$

Per trial calculations

$$Z = \{x_1, x_2, x_3, x_4, x_5, y_1, y_2, y_3, y_4, y_5\}$$

$$\mu_z = \frac{\mu_x + \mu_y}{2}, \sigma_z^2 = \frac{1}{2}(\sigma_x^2 + \sigma_y^2) + \left(\frac{\mu_x - \mu_y}{2}\right)^2$$

The same approach is used when combining the measurements from the two trials, to obtain the statistics for the whole test experiment:

Trial 1 calculation

$$Z1 = \{x_{11}, x_{12}, x_{13}, x_{14}, x_{15}, y_{11}, y_{12}, y_{13}, y_{14}, y_{15}\}$$

$$\mu_{z1}, \sigma_{z1}^2$$

Trial 2 calculations

$$Z2 = \{x_{21}, x_{22}, x_{23}, x_{24}, x_{25}, y_{21}, y_{22}, y_{23}, y_{24}, y_{25}\}$$

$$\mu_{z2}, \sigma_{z2}^2$$



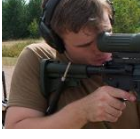
Overall test calculations




$$Test = \{Z1, Z2\}$$

$$\mu_{Test} = \frac{\mu_{z1} + \mu_{z2}}{2}$$




$$\sigma_{Test}^2 = \frac{1}{2}(\sigma_{z1}^2 + \sigma_{z2}^2) + \left(\frac{\mu_{z1} - \mu_{z2}}{2}\right)^2$$

## ANNEX C – Experimental results and calculations

Combat Arms Earplugs Gen IV with OPEN vents									
ATF (Open ears) 		ATF (Closed ears) 			MO / Gunner 				
Time Domain Measurements									
PPL @ eardrum	SEL @ eardrum	PPL @ eardrum	SEL @ eardrum		PPL @ sensor	SEL @ sensor			
158.6 (1)	126.2 (1.3)	126.0(0.8)	96.8(0.8)		156.7(0.6)	123.6(0.7)			
		IPIL							
Sequential T&E Strategy		32.7(1.8)							
Simultaneous T&E Strategy		32.0(1.7)							
Octave Band Measurements									
Open Ear ATF									
Frequency	125Hz	250Hz	500Hz	1000Hz	2000Hz	4000Hz	8000Hz	SPL (eq.28)	
PPL/Oct	119.7	128.2	134.9	147.2	155.8	150.1	137.9	157.4	
$\sigma$ /Oct	0.4	0.6	0.2	0.4	1.7	2.4	2.1		
Closed Ear ATF									
Frequency	125Hz	250Hz	500Hz	1000Hz	2000Hz	4000Hz	8000Hz		
PPL/Oct	109.1	113.2	112.8	116.1	119.5	120.3	109.3		
$\sigma$ /Oct	1.5	1.0	1.8	1.2	1.9	2.4	3.3		
OBIPIL									
Frequency	125Hz	250Hz	500Hz	1000Hz	2000Hz	4000Hz	8000Hz		
OBIPIL	10.7	14.9	22.2	31.1	36.3	29.8	28.6		
OBIPIL BC Corrected									
Frequency	125Hz	250Hz	500Hz	1000Hz	2000Hz	4000Hz	8000Hz		
BC Limits	50	57	61	49	41	50	50		
OBIPIL BC corrected	10.7	14.9	22.2	31.1	36.3	29.8	28.6		
Closed Ear ATF – BC Corrected (Simulating Human Ear)									
Frequency	125Hz	250Hz	500Hz	1000Hz	2000Hz	4000Hz	8000Hz	SPL (eq.28)	
PPL/Oct	109.1	113.2	112.8	116.1	119.5	120.3	109.3	124.7	
								IPIL BC Corrected (eq.29)	32.7
ANE @ MO Location									
ANE (Sequential T&E)		5825		SEL measured at MO location and IPIL derived from the IPIL Sequential T&E strategy.					
ANE (Simultaneous T&E)		4999		SEL measured at MO location and IPIL derived from the IPIL Simultaneous T&E strategy.					
ANE (BC Corrected) (eq.30)		5860		SEL measured at MO location and IPIL BC corrected (Based on Sequential measurements)					

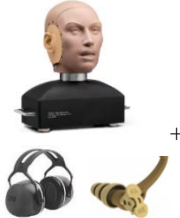
Combat Arms Earplugs Gen IV with CLOSED vents									
ATF (Open ears)			ATF (Closed ears)			MO / Gunner			
									
Time Domain Measurements									
PPL @ eardrum	SEL @ eardrum	PPL @ eardrum	SEL @ eardrum	PPL @ sensor		SEL @ sensor			
158.6(1)	126.2(1.3)	110.9(2.4)	85.2(2.6)	156.7(0.6)		123.6(0.7)			
		IPIL							
Sequential T&E Strategy		47.8(3.2)							
Simultaneous T&E Strategy		47.7(3.3)							
Octave Band Measurements									
Open Ear ATF									
Frequency	125Hz	250Hz	500Hz	1000Hz	2000Hz	4000Hz	8000Hz	SPL (eq.28)	
PPL/Oct	119.7	128.2	134.9	147.2	155.8	150.1	137.9	157.4	
$\sigma$ /Oct	0.4	0.6	0.2	0.4	1.7	2.4	2.1		
Closed Ear ATF									
Frequency	125Hz	250Hz	500Hz	1000Hz	2000Hz	4000Hz	8000Hz		
PPL/Oct	73.5	89.3	93.7	98.3	106.6	105.4	92.4		
$\sigma$ /Oct	8.2	4.0	2.6	1.8	2.1	2.6	3.6		
OBIPIIL									
Frequency	125Hz	250Hz	500Hz	1000Hz	2000Hz	4000Hz	8000Hz		
OBIPIIL	46.2	38.9	41.2	48.9	49.2	44.7	45.5		
OBIPIIL BC Corrected									
Frequency	125Hz	250Hz	500Hz	1000Hz	2000Hz	4000Hz	8000Hz		
BC Limits	50	57	61	49	41	50	50		
OBIPIIL BC corrected	46.2	38.9	41.2	48.9	41.0	44.7	45.5		
Closed Ear ATF – BC Corrected (Simulating Human Ear)									
Frequency	125Hz	250Hz	500Hz	1000Hz	2000Hz	4000Hz	8000Hz	SPL (eq.28)	
PPL/Oct	73.5	89.3	93.7	98.3	114.8	105.4	92.4		
								IPIL BC Corrected (eq.29)	41.9
ANE @ MO Location									
ANE (Sequential T&E)	187828		SEL measured at MO location and IPIL derived from the IPIL Sequential T&E strategy.						
ANE (Simultaneous T&E)	187265		SEL measured at MO location and IPIL derived from the IPIL Simultaneous T&E strategy.						
ANE (BC Corrected) (eq.30)	49183		SEL measured at MO location and IPIL BC corrected (Based on Sequential measurements)						

Superfit 30 EarPlugs								
ATF (Open ears)		ATF (Closed ears)			MO / Gunner			
								
Time Domain Measurements								
PPL @ eardrum	SEL @ eardrum	PPL @ eardrum	SEL @ eardrum	PPL @ sensor		SEL @ sensor		
158.6(1)	126.2(1.3)	111.8(1.3)	86.6(2.5)	156.7(0.6)		123.6(0.7)		
		IPIL						
Sequential T&E Strategy		46.9(2.1)						
Simultaneous T&E Strategy		45.8(2.2)						
Octave Band Measurements								
Open Ear ATF								
Frequency	125Hz	250Hz	500Hz	1000Hz	2000Hz	4000Hz	8000Hz	SPL(eq.28)
PPL/Oct	119.7	128.2	134.9	147.2	155.8	150.1	137.9	157.4
$\sigma$ /Oct	0.4	0.6	0.2	0.4	1.7	2.4	2.1	
Closed Ear ATF								
Frequency	125Hz	250Hz	500Hz	1000Hz	2000Hz	4000Hz	8000Hz	
PPL/Oct	84.6	90.1	90.1	98.9	109.3	104.0	89.5	
$\sigma$ /Oct	6.3	2.1	1.4	0.9	2.4	2.3	3.5	
OBIPIL								
Frequency	125Hz	250Hz	500Hz	1000Hz	2000Hz	4000Hz	8000Hz	
OBIPIL	35.2	38.1	44.8	48.3	46.6	46.1	48.4	
OBIPIL BC Corrected								
Frequency	125Hz	250Hz	500Hz	1000Hz	2000Hz	4000Hz	8000Hz	
BC Limits	50	57	61	49	41	50	50	
OBIPIL BC corrected	35.2	38.1	44.8	48.3	41.0	46.1	48.4	
Closed Ear ATF – BC Corrected (Simulating Human Ear)								
Frequency	125Hz	250Hz	500Hz	1000Hz	2000Hz	4000Hz	8000Hz	SPL(eq.28)
PPL/Oct	84.6	90.1	90.1	98.9	114.8	104.0	89.5	115.3
							IPIL BC Corrected (eq.29)	42.1
ANE @ MO Location								
ANE (Sequential T&E)	153017		SEL measured at MO location and IPIL derived from the IPIL Sequential T&E strategy.					
ANE (Simultaneous T&E)	120504		SEL measured at MO location and IPIL derived from the IPIL Simultaneous T&E strategy.					
ANE (BC Corrected) (eq.30)	50753		SEL measured at MO location and IPIL BC corrected (Based on Sequential measurements)					

X5A ear muff								
ATF (Open ears)		ATF (Closed ears)				MO / Gunner		
								
Time Domain Measurements								
PPL @ eardrum	SEL @ eardrum	PPL @ eardrum	SEL @ eardrum	PPL @ sensor	SEL @ sensor			
158.3(0.8)	125.7(1.1)	120.5(1.8)	94.3(0.5)	156.7(0.6)	123.6(0.7)			
IPIL								
Sequential T&E Strategy		37.8(2.3)						
Simultaneous T&E Strategy		38.1(2.2)						
Octave Band Measurements								
Open Ear ATF								
Frequency	125Hz	250Hz	500Hz	1000Hz	2000Hz	4000Hz	8000Hz	SPL(eq.28)
PPL/Oct	119.8	128.2	135.3	147.3	155.7	148.2	135.9	
$\sigma$ /Oct	0.7	1.0	0.4	0.6	1.9	2.1	2.0	
Closed Ear ATF								
Frequency	125Hz	250Hz	500Hz	1000Hz	2000Hz	4000Hz	8000Hz	
PPL/Oct	108.4	104.3	99.2	99.3	117.3	107.2	102.0	
$\sigma$ /Oct	0.8	0.9	1.0	1.0	2.1	3.9	2.7	
OBIPIIL								
Frequency	125Hz	250Hz	500Hz	1000Hz	2000Hz	4000Hz	8000Hz	
OBIPIIL	11.4	23.9	36.1	48.0	38.4	41.0	33.9	
OBIPIIL BC Corrected								
Frequency	125Hz	250Hz	500Hz	1000Hz	2000Hz	4000Hz	8000Hz	
BC Limits	50	57	61	49	41	50	50	
OBIPIIL BC corrected	11.4	23.9	36.1	48.0	38.4	41.0	33.9	
Closed Ear ATF – BC Corrected (Simulating Human)								
Frequency	125Hz	250Hz	500Hz	1000Hz	2000Hz	4000Hz	8000Hz	SPL (eq.28)
PPL/Oct	108.4	104.3	99.2	99.3	117.3	107.2	102.0	118.5
IPIL BC Corrected (eq.29)								38.4
ANE @ MO Location								
ANE (Sequential T&E)	19125		SEL measured at MO location and IPIL derived from the IPIL Sequential T&E strategy.					
ANE (Simultaneous T&E)	20344		SEL measured at MO location and IPIL derived from the IPIL Simultaneous T&E strategy.					
ANE (BC Corrected) (eq.30)	21813		SEL measured at MO location and IPIL BC corrected (Based on Sequential measurements)					

X5A earmuff combined with Combat Arm earplugs (Open vents)									
ATF (Open ears)		ATF (Closed ears)				MO / Gunner			
									
Time Domain Measurements									
PPL @ eardrum	SEL @ eardrum	PPL @ eardrum	SEL @ eardrum		PPL @ sensor		SEL @ sensor		
157.2(1.5)	125.0(2.2)	111.5(6.8)	89.6(5.7)		156.7(0.6)		123.6(0.7)		
		IPIL							
Sequential T&E Strategy		44.1(1.9)							
Simultaneous T&E Strategy		45.0(1.3)							
Octave Band Measurements									
Open Ear ATF									
Frequency	125Hz	250Hz	500Hz	1000Hz	2000Hz	4000Hz	8000Hz	SPL (eq.28)	
PPL/Oct	118.5	127.4	134.2	146.5	153.8	148.0	133.7	155.5	
$\sigma$ /Oct	0.6	0.9	0.8	1.2	3.6	2.6	1.5		
Closed Ear ATF									
Frequency	125Hz	250Hz	500Hz	1000Hz	2000Hz	4000Hz	8000Hz		
PPL/Oct	105.1	97.7	96.7	93.6	86.0	79.8	79.6		
$\sigma$ /Oct	6.4	9.1	13.0	13.7	6.3	6.1	7.1		
OBIPIIL									
Frequency	125Hz	250Hz	500Hz	1000Hz	2000Hz	4000Hz	8000Hz		
OBIPIIL	13.4	29.7	37.5	52.9	67.8	68.2	54.1		
OBIPIIL BC Corrected									
Frequency	125Hz	250Hz	500Hz	1000Hz	2000Hz	4000Hz	8000Hz		
BC Limits	50	57	61	49	41	50	50		
OBIPIIL BC corrected	13.4	29.7	37.5	49.0	41.0	50.0	50.0		
Closed Ear ATF – BC Corrected (Simulating Human)									
Frequency	125Hz	250Hz	500Hz	1000Hz	2000Hz	4000Hz	8000Hz	SPL (eq.28)	
PPL/Oct	105.1	97.7	96.7	97.5	112.8	98.0	83.7	113.9	
								IPIL BC Corrected (eq.29)	41.6
ANE @ MO Location									
ANE (Sequential T&E)		80716		SEL measured at MO location and IPIL derived from the IPIL Sequential T&E strategy.					
ANE (Simultaneous T&E)		98581		SEL measured at MO location and IPIL derived from the IPIL Simultaneous T&E strategy.					
ANE (BC Corrected) (eq.30)		45330		SEL measured at MO location and IPIL BC corrected (Based on Sequential measurements)					

X5A earmuff combined with Combat Arm earplugs (Closed vents)									
ATF (Open ears)		ATF (Closed ears)				MO / Gunner			
									
Time Domain Measurements									
PPL @ eardrum	SEL @ eardrum	PPL @ eardrum		SEL @ eardrum		PPL @ sensor		SEL @ sensor	
157.2(1.5)	125.0(2.2)	99.5(6.2)		81.6(6.7)		156.7(0.6)		123.6(0.7)	
		IPIL							
Sequential T&E Strategy		52.2(2.1)							
Simultaneous T&E Strategy		53.0(1)							
Octave Band Measurements									
Open Ear ATF									
Frequency	125Hz	250Hz	500Hz	1000Hz	2000Hz	4000Hz	8000Hz	SPL (eq.28)	
PPL/Oct	118.5	127.4	134.2	146.5	153.8	148.0	133.7	155.5	
$\sigma$ /Oct	0.6	0.9	0.8	1.2	3.6	2.6	1.5		
Closed Ear ATF									
Frequency	125Hz	250Hz	500Hz	1000Hz	2000Hz	4000Hz	8000Hz		
PPL/Oct	74.7	86.7	86.4	84.2	81.9	77.2	75.4		
$\sigma$ /Oct	6.0	9.3	17.2	16.2	12.2	7.0	8.4		
OBIPIIL									
Frequency	125Hz	250Hz	500Hz	1000Hz	2000Hz	4000Hz	8000Hz		
OBIPIIL	43.7	40.7	47.8	62.3	71.9	70.8	58.3		
OBIPIIL BC Corrected									
Frequency	125Hz	250Hz	500Hz	1000Hz	2000Hz	4000Hz	8000Hz		
BC Limits	50	57	61	49	41	50	50		
OBIPIIL BC corrected	43.7	40.7	47.8	49.0	41.0	50.0	50.0		
Closed Ear ATF – BC Corrected (Simulating Human Ear)									
Frequency	125Hz	250Hz	500Hz	1000Hz	2000Hz	4000Hz	8000Hz	SPL (eq.28)	
PPL/Oct	74.7	86.7	86.4	97.5	112.8	98.0	83.7	113.1	
								IPIL BC Corrected (eq.29)	42.4
ANE @ MO Location									
ANE (Sequential T&E)	526990		SEL measured at MO location and IPIL derived from the IPIL Sequential T&E strategy.						
ANE (Simultaneous T&E)	631552		SEL measured at MO location and IPIL derived from the IPIL Simultaneous T&E strategy.						
ANE (BC Corrected) (eq.30)	54660		SEL measured at MO location and IPIL BC corrected (Based on Sequential measurements)						

X5A earmuff combined with Superfit 30 EarPlugs									
ATF (Open ears)		ATF (Closed ears)				MO / Gunner			
									
Time Domain Measurements									
PPL @ eardrum	SEL @ eardrum	PPL @ eardrum		SEL @ eardrum		PPL @ sensor		SEL @ sensor	
157.2(1.5)	125.0(2.2)	95.9(3.9)		80.0(2.3)		156.7(0.6)		123.6(0.7)	
		<b>IPIL</b>							
Sequential T&E Strategy		58.1(1.9)							
Simultaneous T&E Strategy		59.9(3.3)							
Octave Band Measurements									
Open Ear ATF									
Frequency	125Hz	250Hz	500Hz	1000Hz	2000Hz	4000Hz	8000Hz	SPL (eq.28)	
PPL/Oct	118.5	127.4	134.2	146.5	153.8	148.0	133.7	155.5	
$\sigma$ /Oct	0.6	0.9	0.8	1.2	3.6	2.6	1.5		
Closed Ear ATF									
Frequency	125Hz	250Hz	500Hz	1000Hz	2000Hz	4000Hz	8000Hz		
PPL/Oct	79.1	84.3	82.3	79.4	78.0	74.7	73.2		
$\sigma$ /Oct	2.9	4.3	4.7	4.5	6.9	5.9	6.0		
OBIPIIL									
Frequency	125Hz	250Hz	500Hz	1000Hz	2000Hz	4000Hz	8000Hz		
OBIPIIL	39.4	43.1	51.9	67.1	75.8	73.3	60.5		
OBIPIIL BC Corrected									
Frequency	125Hz	250Hz	500Hz	1000Hz	2000Hz	4000Hz	8000Hz		
BC Limits	50	57	61	49	41	50	50		
OBIPIIL BC corrected	39.4	43.1	51.9	49.0	41.0	50.0	50.0		
Closed Ear ATF – BC Corrected (Simulating Human Ear)									
Frequency	125Hz	250Hz	500Hz	1000Hz	2000Hz	4000Hz	8000Hz	SPL (eq.28)	
PPL/Oct	79.1	84.3	82.3	97.5	112.8	98.0	83.7	113.1	
								<b>IPIL BC Corrected (eq.29)</b>	<b>42.4</b>
ANE @ MO Location									
ANE (Sequential T&E)	2037080		SEL measured at MO location and IPIL derived from the IPIL Sequential T&E strategy.						
ANE (Simultaneous T&E)	3076305		SEL measured at MO location and IPIL derived from the IPIL Simultaneous T&E strategy.						
ANE (BC Corrected) (eq.30)	54772		SEL measured at MO location and IPIL BC corrected (Based on Sequential measurements)						

## ANNEX D – CAF hearing conservation requirements when using a 5.56 mm caliber firearm

### General.

It was confirmed with the U. of Ottawa Office of Research Ethics and Integrity and the U. of Ottawa Office of Risk Management that since the project did not involve measuring the effects of sounds on personnel, and since the project measurements are being conducted on DND sites, exclusively by DND personnel wearing adequate hearing protection and following proper safety procedures, it was not required to obtain additional certification for this project from the U. of Ottawa Research Ethics Board.

### CAF hearing conservation requirements.

Impulse noise of sufficient magnitude is hazardous to hearing. Guidelines have been developed for hearing conservation. The operational requirements for a safe training are detailed by the CAF operational training safety requirements [62] and provided in this annex for the case when the used firearm is a 5.56 mm caliber firearm. Military Operators must apply these requirements to avoid hearing damage.

**Protection.** All weapon firing and demolitions are potentially hazardous to hearing. Personnel will only wear aural protection that is authorized for use on that particular range. Any person in close proximity to demolition charges or weapons that are being fired shall wear a properly fitted hearing protection device as follows:

- a. Ear Plugs. All personnel engaged in training or administrative duties on live firing ranges must insert foam earplug. These plugs will be worn as a minimum protective device when firing practices are being conducted, including the firing of blank artillery ammunition.
- b. Aural Protectors. Although not generally as effective at reducing noise as foam earplugs, aural protectors (also known as earmuffs) may be worn when frequent removal and refitting are required, or when the use of earplugs makes it difficult to understand verbal commands. For slightly better protection, earmuffs shall be worn in combination with plugs for daily maximum exposure limits.

**Summary.** The following table summarizes the hearing protection required for a 5.56 mm small firearm as per [62].

CAF Maximum daily exposure rates for a 5.56 mm small firearm					
Noise Source	Position	ANE			
		Without protection	Ear Muffs	Ear plugs	Both
Rifle, C7, 5.56 mm, outdoor range	Shooter	4	30	270	540